Evaluating the Environmental Criticality of Massive Objects in LEO for Debris Mitigation and Remediation

Carmen Pardini[a]*, Luciano Anselmo[a]•

[a] *Space Flight Dynamics Laboratory, Institute of Information Science and Technologies (ISTI), National Research Council (CNR), Via G. Moruzzi 1, 56124 Pisa, Italy*

* carmen.pardini@isti.cnr.it

• luciano.anselmo@isti.cnr.it

Abstract

Approximately 95% of the mass in Earth orbit is currently concentrated in about 6700 intact objects, of which nearly 80% are abandoned and more than 90% cannot be maneuvered. The intact objects abandoned in low Earth orbit (LEO) above 650 km, i.e. with an average residual lifetime of more than 25 years, represent the main potential mass reservoir for the generation of new detrimental orbital debris in case of mutual collisions with the existing debris environment, taking into account that an 800 g impactor may be sufficient, in principle, to shatter a 1000 kg spacecraft or rocket stage. Since the 1980's, several mitigation measures were promoted and agreed at the international level in order to prevent the occurrence of new breakups in space and put under control the accumulation of mass abandoned in orbit, but unfortunately the level of compliance with such guidelines, requirements or standards is still far from satisfactory. Moreover, the appearance on the scene of space activity of new private and government actors from a growing number of countries makes the proper management of the circumterrestrial space a task of increasing complexity, taking also into account the rapid emerging of new potential applications, disrupting technologies and operational approaches quite different from the past. In this rapidly evolving environment, it might be useful to have a simple and flexible instrument for evaluating the potential criticality for the environment of massive objects placed or abandoned in LEO. With this goal, in the last few years, a particular effort was devoted to the development of various "criticality indexes", then applied for evaluating many families of rocket bodies and selected spacecraft. In this paper, with the underlining ambition to be simple, intuitive and relevant, from an environmental point of view, a couple of the most complete indexes were coherently applied in order to assess the potential criticality of the most massive objects abandoned in LEO. The results obtained are presented here in detail, also highlighting how these ranking approaches might be used both for debris mitigation, for instance to choose an appropriate disposal orbit for either spacecraft or upper stages to be dismissed at the end-of-life, and for debris remediation, as a guide in the selection of the most relevant targets for active debris removal, if and when such missions will become practicable.

Keywords: space debris, criticality index, intact objects, low Earth orbit, mitigation, remediation ranking.

1. Introduction

The long-term simulations of the orbital debris environment carried out during the last 40 years have identified the abandoned mass in orbit as the main driver of collisional fragments and impact probability growth over several decades, potentially jeopardizing the practical utilization of some of the most popular orbital regimes, particularly in low Earth orbit (LEO) [1,2]. For this reason, a "25-year rule", i.e. the prescription of limiting to less than 25 years the post-mission orbital presence of spacecraft and orbital stages in LEO, was firstly suggested inside the National Aeronautics and Space Administration (NASA), later on endorsed by the Inter-Agency Space Debris Coordination Committee (IADC), and finally adopted by several national and international standards [3]. The aim of the rule was averting the accumulation of intact spacecraft and orbital stages, in order to retard as much as possible a rapid growth of artificial debris

and collision rates triggered by mutual collisions and catastrophic breakups [4,5].

Presently there are approximately 7500 metric tons of mass in orbit around the Earth, of which about 95% concentrated in almost 6700 intact spacecraft and orbital stages [6]. Among them, nearly 80% are abandoned and more than 90% cannot be maneuvered. Those left above ~ 650 km, i.e. with a typical residual lifetime of more than 25 years, represent the main potential mass reservoir for the generation of new detrimental orbital debris in case of mutual collisions with the existing debris environment, taking into account that an 800 g impactor may be sufficient, in principle and on average, to deeply shatter a 1000 kg spacecraft or rocket stage. Just considering the most massive objects abandoned in LEO, the 9000 kg second stages of the Zenit-2 launcher, it has been pointed out that there is a 1/4000 probability per year of a collision involving two of them, leading to an immediate doubling of the cataloged debris population in LEO [7].

A possible approach for gauging the latent long-term environmental impact of an orbiting object, avoiding thousands of complex simulations built on rather uncertain scenario assumptions and forecasts [8], is to formulate a "criticality index" grounded on simplified credible assumptions and characterized by much faster, and easier to implement, computations. An intuitive and simple to understand meaning, if possible, would add further practical value to the definition, which may represent, for instance, a good starting point for the assessment of the post-mission disposal options for a spacecraft or an orbital stage, or for a preliminary analysis of environmental criticality and prioritization of intact targets for active debris removal (ADR). An appropriately defined criticality index may be therefore beneficial both for mitigation and remediation debris evaluations.

During the last decade, several criticality/ranking indexes have been proposed [9-17]. In this paper, the definition presented in [18-20] was adopted. A simplified version of it, particularly suited for analyzing relatively homogeneous sets of objects, had been previously and extensively used for the relative ranking in between and among the main families of rocket bodies [21,22]. However, being this work devoted to both spacecraft and orbital stages, the use of the complete index defined in [18-20] was deemed more appropriate.

The analysis presented in the following considered all the unclassified intact objects fully resident in LEO, i.e. with a mean altitude ≤ 2000 km, with a perigee height ≥ 650 km and with a mass ≥ 1000 kg, as of 3 May 2017. This included 165 spacecraft, with a total mass of about 325 metric tons, and 434 rocket bodies, with a total mass of about 801 metric tons. Together, with 1126 metric tons, accounted for 40% of the total mass of intact objects in LEO, including the International Space Station, and 47% excluding the permanent human habitat [23]. The analysis was also extended to constellation satellites with an individual mass < 1000 kg, but characterized by a mean altitude > 900 km. The constellations considered, in order of decreasing total mass, were the following: Parus, Globalstar, Strela 3, Strela 1M, Tsiklon, Tsikada, Sfera, Yaogan[†], and Gonets (Fig.1). In total, 737 spacecraft, with a total mass approaching 208 metric tons.

In conclusion, all the objects included in the study had a combined mass of 1334 metric tons, i.e. 47% of the total mass of intact objects in LEO, including the International Space Station, and 56% excluding it. Moreover, most of the ignored mass orbited below 650 km, so was not relevant for the long-term evolution of the debris environment, due to the cleaning effect of thermospheric drag. Therefore, the selection criteria adopted should have sorted out almost all, if not all, the most critical objects in LEO potentially able to play an adverse role on the long-term evolution of the debris environment.

[†]The Yaogan satellites listed here were those with mass < 1000 kg; the other ones with mass exceeding one metric ton were instead included in the general analysis.

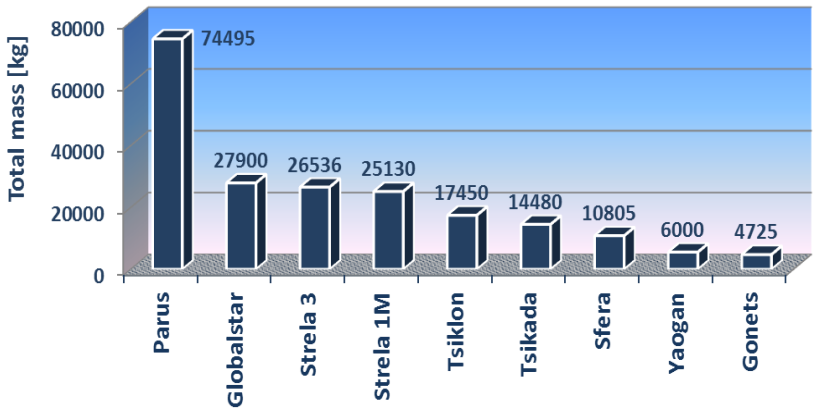

Fig. 1. Constellation satellites in LEO with an individual mass <1000 kg and a mean height >900 km, in order of decreasing total mass

2. Criticality index setup

The criticality index (R) adopted in this study was already introduced and described in detail elsewhere [18-20]. However, in order to improve the readability of the paper, review all the assumptions made and pointing out the small fine tunings introduced, the definition is recalled in the following.

Starting from the idea that a higher criticality index should be associated with a greater potential for adverse effects on the LEO debris environment, its building began with the product of two functions, f and g, the first one depending on the probability of catastrophic fragmentation P_c due to orbital debris collision, and on the number of new "projectiles" N_p resulting from the breakup, the second one characterizing the long-term impact on the environment as a function of the lifetime of the new cloud of fragments, of the volume of space involved, and of the interaction with the pre-existing debris distribution:

$$R = f \cdot g \tag{1}$$

Taking into account that the condition $P_c < 0.1$ generally applies and that the typical "critical projectiles" are ~ 20 times smaller than the targets, the probability of catastrophic collisional fragmentation can be expressed, in terms of the flux of debris $F(t)$ able to destroy the target object, of the average cross-section A of the latter, and of the interval of time t considered, as follows:

$$P_c \approx \int F(t) \cdot A \cdot dt \tag{2}$$

However, being the time evolution of $F(t)$ affected by significant uncertainties [8], and the computation of the integral for each specific target object quite cumbersome, also because the flux of debris leading to a catastrophic fragmentation, i.e. with masses $\geq m_D(M)$, is a function of the target mass M, orbit inclination i and altitude h as well, it was decided of including in the definition just the current flux $F = F\left[h, i, m_D(M)\right]$, either provided by a debris model or estimated using a catalog. This led to:

$$P_c \sim F\left[h, i, m_D(M)\right] \cdot A \cdot L_T \tag{3}$$

where L_T is the object residual lifetime, approximated as the product between the object mass-to-area ratio M/A and a "normalized" mean lifetime function $l(h)$:

$$L_T \cong l(h) \cdot \frac{M}{A} \tag{4}$$

Fig. 2 shows the mean lifetime function $L_{T0}(h)$ computed for an average intact object in LEO, as could be found in mid-2013 [8,12,24], with $M_0 = 934$ kg and $A_0 = 11$ m^2. The "normalized" mean lifetime function $l(h)$ can be therefore written in the following way:

$$l(h) = L_{T0}(h) \cdot \frac{A_0}{M_0} \tag{5}$$

leading to:

$$P_c \sim F\left[h, i, m_D(M)\right] \cdot l(h) \cdot M \tag{6}$$

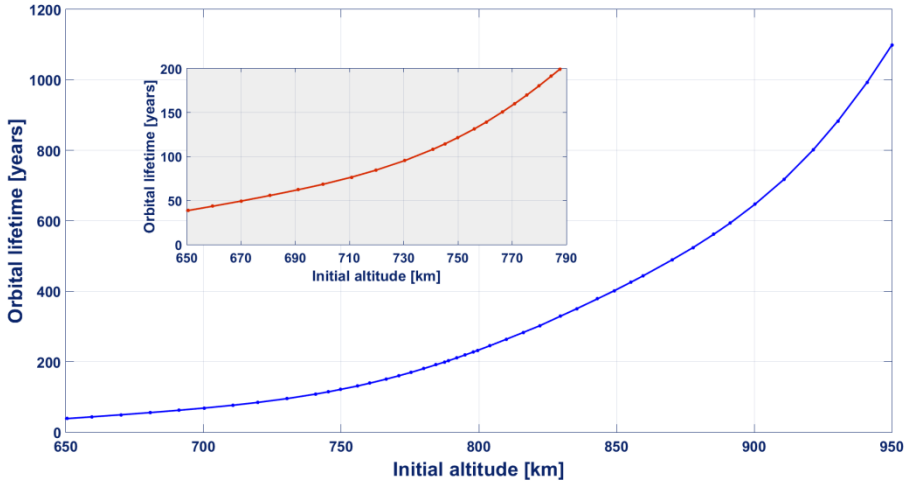

Fig. 2. Mean orbital lifetime, as a function of the initial altitude in nearly circular orbit, of an average intact object

In order to quantify the number of new "projectiles" resulting from a hypothetical disrupting collision, the NASA standard breakup model was used [25,26]. In it, the cumulative number of fragments N_p generated in a catastrophic collision and larger than a given characteristic size is proportional to the cumulative mass of the target object and the impacting debris, raised to the 0.75th power. It should be however pointed out that, in most of the cases, the cumulative mass would be in practice very close to the target mass, being the latter generally much larger (by 3 orders of magnitude in LEO) than the impactor's one. As a result, $N_p \propto M^{0.75}$, leading to the following expression for the f function:

$$f \equiv P_c \cdot M^{0.75} \sim F\left[h, i, m_D(M)\right] \cdot l(h) \cdot M^{1.75} \tag{7}$$

Regarding the definition of the g function, the first step was the evaluation of the long-term impact on the environment of the new debris cloud resulting from a potential catastrophic collision. It was therefore introduced the concept of collisional debris cloud decay of 50% of the catalogable fragments (*CDCD*50). Given a collisional cloud of fragments with sizes $d \geq 10$ cm, released around a certain mean altitude, its *CDCD*50 represents the time needed for the orbital decay of 50% of the pieces due to air drag. In other words, *CDCD*50 is the cloud half-life. Fig. 3 shows *CDCD*50 as a function of the mean breakup altitude in

nearly circular orbit. It was calibrated studying the area-to-mass distribution and orbital evolution of the cloud of cataloged fragments resulting from the catastrophic collisional destruction of the Cosmos 2251 satellite, on 10 February 2009 [27].

Coming to the volume of space affected by the potential breakup and to the interaction of the resulting fragment cloud with the pre-existing debris distribution, the choice fell on the ratio between the flux of debris able to induce a catastrophic fragmentation, i.e. with masses $\geq m_D(M)$, at the target mean altitude h and orbital inclination i, and the flux at the same altitude, but for $i = 0°$. This z function was therefore defined in the following way:

$$z\left[h,i,m_D(M)\right] \equiv \frac{F\left[h,i,m_D(M)\right]}{F\left[h,i=0°,m_D(M)\right]} \tag{8}$$

Such approximately bell shaped function in LEO peaks around polar inclinations and has minima for equatorial, or nearly equatorial, orbits, either direct or retrograde. [18-20].

Then, the g function can be defined as follows:

$$g \equiv CDCD50(h) \cdot z\left[h,i,m_D(M)\right] \tag{9}$$

completing the intended set up of the criticality index R, which becomes:

$$R \equiv F(h,i,m_D) \cdot l(h) \cdot M^{1.75} \cdot CDCD50(h) \cdot z(h,i,m_D) \tag{10}$$

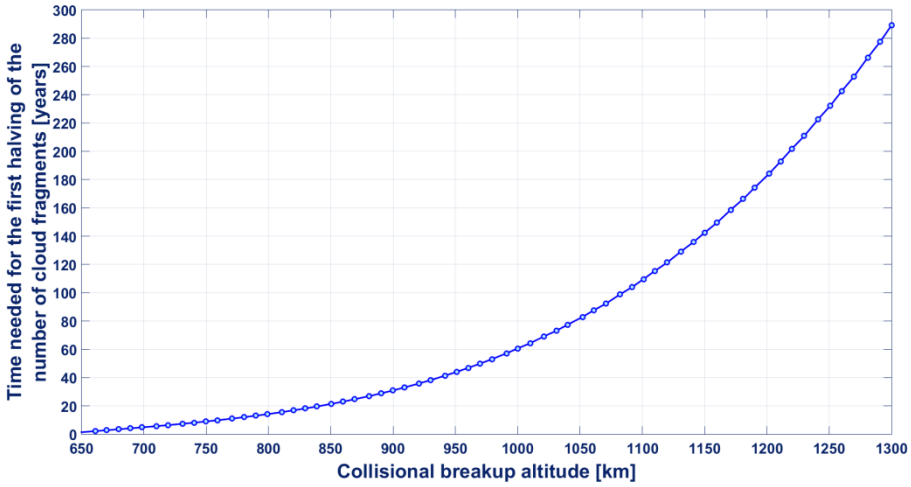

Fig. 3. First halving time of the number of catalogable debris generated by a catastrophic collision (CDCD50), as a function of the breakup altitude in nearly circular orbit

3. Normalized and dimensionless criticality index

For practical applications, it was highly desirable deriving a criticality index R_N both normalized and dimensionless. Therefore, the average intact object in LEO, as of mid-2013 [12,24], was used for defining a reference object, with $M_0 = 934$ kg, placed into a circular sun-synchronous orbit with $h_0 = 800$ km and $i_0 = 98.5°$. The normalized and dimensionless criticality index R_N was then defined in the following way:

$$R_N \equiv \frac{F\left[h,i,m_D(M)\right]}{F\left[h_0,i_0,m_D(M_0)\right]} \cdot \frac{l(h)}{l(h_0)} \cdot \left(\frac{M}{M_0}\right)^{1.75} \times \frac{CDCD50(h)}{CDCD50(h_0)} \cdot \frac{z\left[h,i,m_D(M)\right]}{z\left[h_0,i_0,m_D(M_0)\right]} \tag{11}$$

where it was set:

$$l(h) / l(h_0) \equiv 1 \text{ when } h > h_0 \tag{12}$$

and:

$$\frac{CDCD50(h > 1250\text{km})}{CDCD50(h = 1250\text{km})} \equiv 1 \tag{13}$$

These conditions, corresponding, in the case of Eq. (12), to an orbital lifetime equal or greater than about 230 years for the target object (see Fig. 2), and, in the case of Eq. (13), to a half-life equal or greater than about 230 years for the possible debris cloud (see Fig. 3), were introduced to avoid of giving too much weight, in relative terms, to objects with very long lifetimes, much longer, in fact, than any reasonable temporal horizon for the current modeling, technology and social projections. Moreover, having adopted for the index definition a normalized and dimensionless ratio instead of an absolute value, R_N is nearly independent from the specific assumptions used to build the $l(h)$ and the $CDCD50$ functions.

4. Study targets and assumptions

As anticipated in Section 1, the study considered all the unclassified intact spacecraft and orbital stages fully resident in LEO, as of 3 May 2017 (Fig. 4), with a perigee height ≥ 650 km and with a mass ≥ 1000 kg. In addition, it also analyzed the constellation satellites with an individual mass < 1000 kg and a mean height > 900 km (Fig. 1).

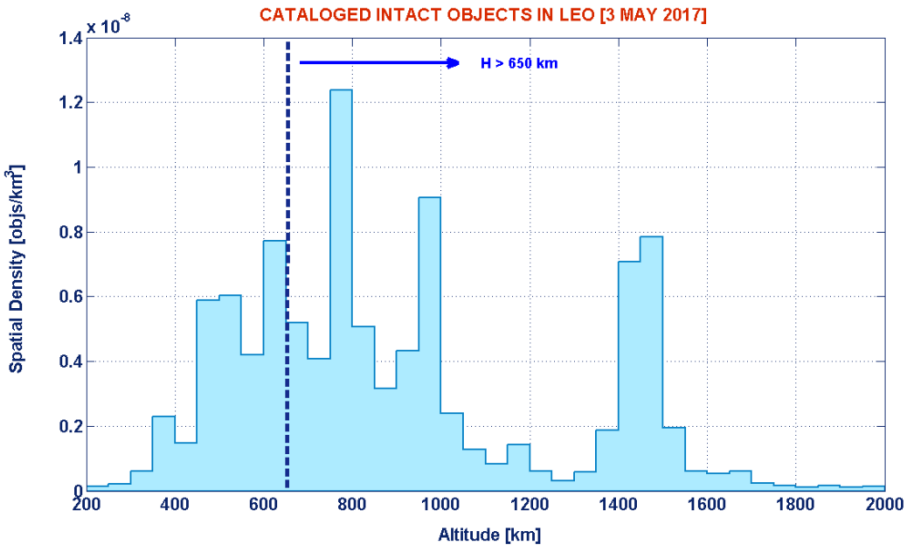

Fig. 4. Spatial density, in objects per km³, of cataloged intact objects in LEO, as of 3 May 2017

The debris mass $m_D(M)$ able to produce the catastrophic breakup of a target object of mass M was estimated by assuming a mean relative velocity of 10 km/s [28,29] and a specific fragmentation energy of 40 000 J/kg [30]. The flux of orbital debris having mass ≥ $m_D(M)$, i.e. $F\,[h,i,m_D(M)]$, was computed using

the SDIRAT tool [29,32], applied to the MASTER-2009 population model [31].

All the computations were repeated using the catalog of the unclassified orbital objects issued by the US Strategic Command on 3 May 2017. In that case, the flux, F_{cat} (h,i), was again computed with SDIRAT, using the population of all cataloged objects, irrespective of their masses. This led to the estimation of the criticality index R_{Ncat}:

$$R_{Ncat} \equiv \frac{F_{cat}(h,i)}{F_{cat}(h_0,i_0)} \cdot \frac{l(h)}{l(h_0)} \cdot \left(\frac{M}{M_0} \right)^{1.75} \times \frac{CDCD50(h)}{CDCD50(h_0)} \cdot \frac{z_{cat}(h,i)}{z_{cat}(h_0,i_0)} \tag{14}$$

The reasons for computing also an index like R_{Ncat} were the following:

1. Large space objects, made of two or more nearly structurally independent modules, or having pressurized tanks, just to highlight a couple of examples, might suffer a catastrophic breakup even if hit by debris with mass < $m_D(M)$ [24];
2. Collisions among cataloged objects are anyway relevant events;
3. The debris catalog is updated daily, while a population model requests years to be developed and validated;
4. If the ranking order obtained with R_N is basically the same obtained with R_{Ncat}, the latter is much easier and straightforward to compute.

5. Criticality of spacecraft

The values of R_N and R_{Ncat} obtained for the 165 spacecraft in LEO with perigee height ≥ 650 km and mass ≥ 1000 kg are summarized in Figs. 5-14. R_N (MASTER) is always plotted in brown, R_{Ncat} (CATALOG) is always plotted in blue. The satellites with a "*" superscript were still functioning when the analysis was carried out, so their criticality indexes were applicable to the operational orbit, in case of no de-orbiting at the end-of-life. Tables A.1-A.8, in Appendix A, show the mean altitude, inclination and mass for each of the 165 spacecraft considered in this analysis.

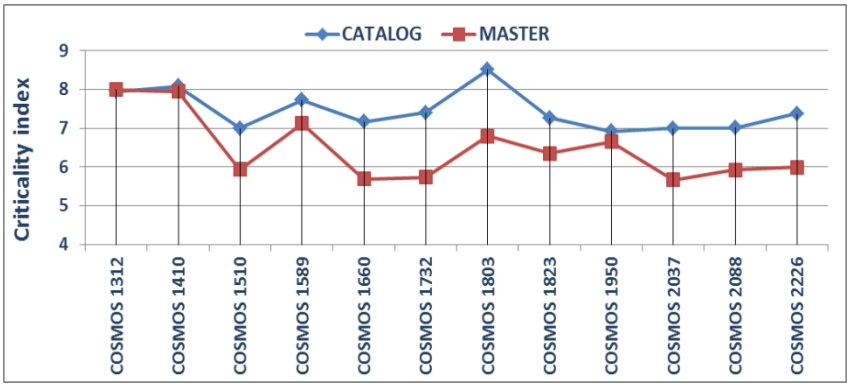

Fig. 5. Criticality index of the Russian Geo-IK geodesy satellites (M = 1500 kg), Table A.1

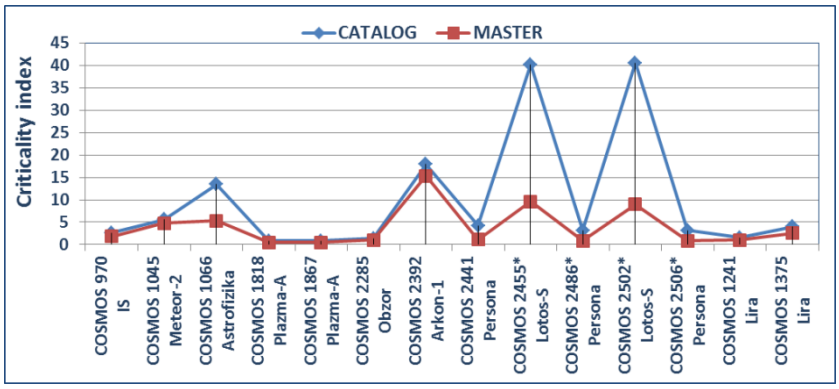

Fig. 6. Criticality index of heterogeneous Cosmos satellites, with mass up to 7000 kg (Cosmos 2441, 2455 and 2502), Table A.2

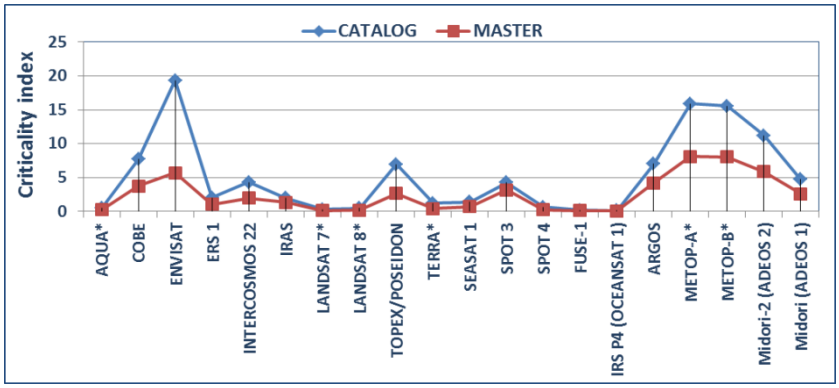

Fig. 7. Criticality index of heterogeneous satellites from Europe, United States and Japan, with mass up to 8110 kg (Envisat), Table A.3

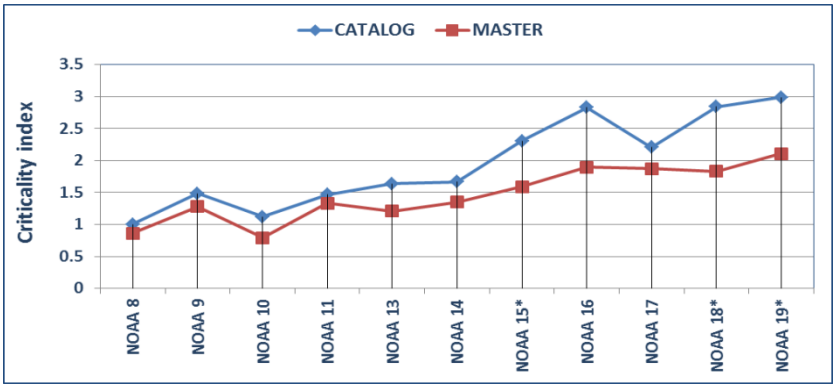

Fig. 8. Criticality index of NOAA meteorological satellites, with mass up to 1441 kg (NOAA 15), Table A.4

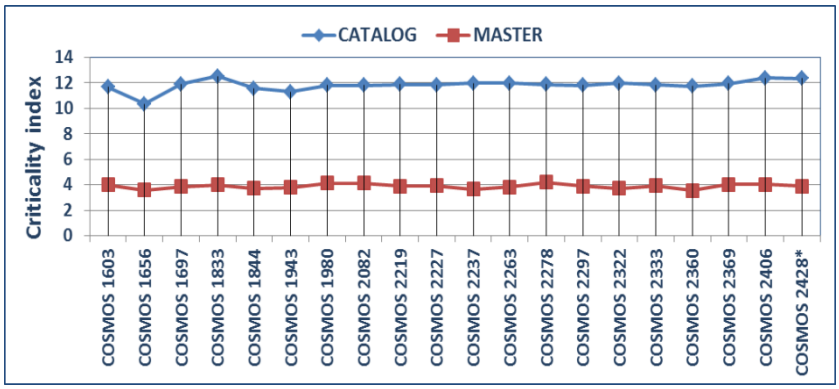

Fig. 9. Criticality index of the Russian Tselina-2 electronic intelligence satellites ($M \approx 3200$ kg), Table A.5

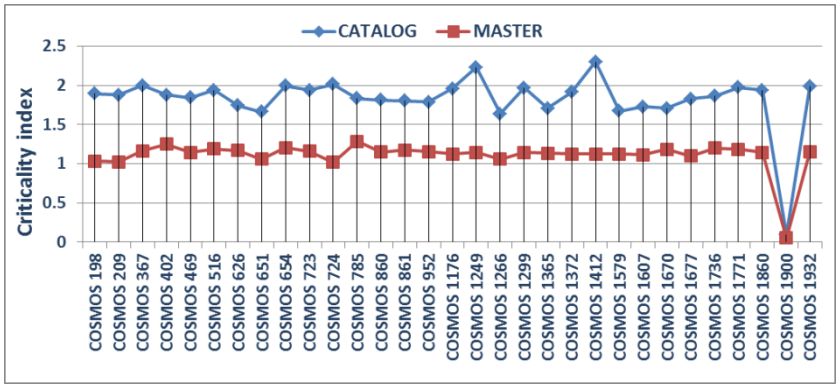

Fig. 10. Criticality index of the Russian US-A radar ocean reconnaissance satellites (RORSAT, $M = 1250$ kg), Table A.6

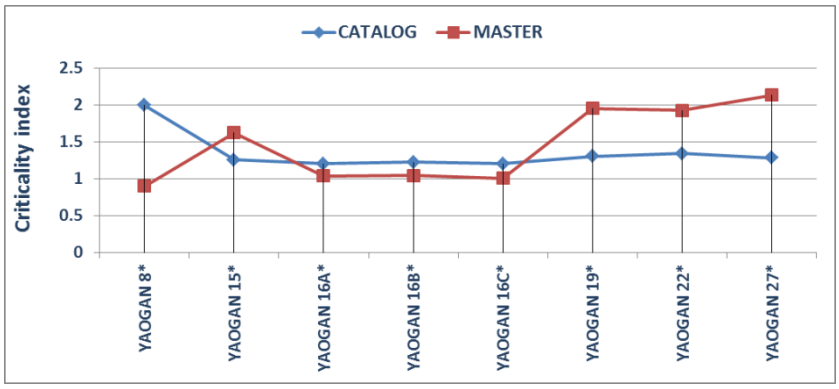

Fig. 11. Criticality index of the Chinese Yaogan reconnaissance satellites with a mass greater than one metric ton ($M = 1040$ kg), Table A.7

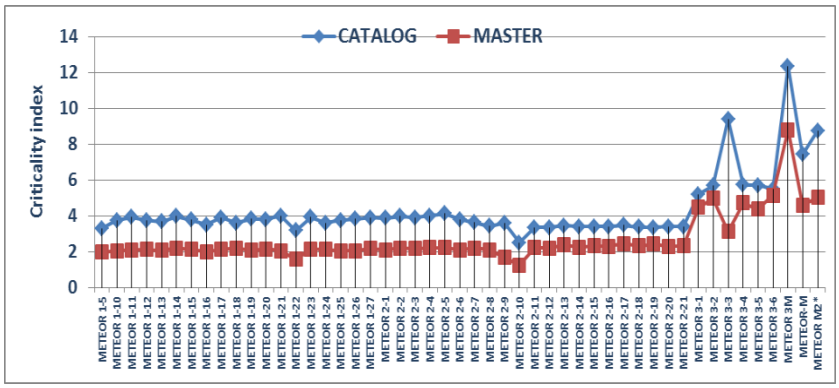

Fig. 12. Criticality index of the Russian Meteor meteorological satellites, with mass up to 2900 kg (Meteor M2), Table A.8

No criticality index greater than one was obtained below 700 km, while above 800 km all the objects considered had an index close to one or greater (Fig. 14). Among the operational spacecraft, the highest values were found for the Lotos-S satellites Cosmos 2455 and 2502, and for the meteorological satellites Metop A and B, and Meteor M2 (Fig. 13). Among the abandoned spacecraft, the most critical objects resulted to be Cosmos 2392 (Arkon-1), the Geo-IK geodesy satellites, several meteorological Meteor satellites (Cosmos 1045 and Meteor 3-1, 3-2, 3-4, 3-5, 3-6, 3M, and M), Midori 2 (ADEOS 2), Envisat, Cosmos 1066 (Astrofizika), ARGOS and the Tselina-2 satellites (Fig. 13).

As illustrated in Fig. 15, $R_N > 1$ was found for 148 satellites, $R_N > 2$ for 93, $R_N > 3$ for 53, $R_N > 4$ for 36, $R_N > 5$ for 23, and $R_N > 10$ for only one spacecraft (Cosmos 2392). $R_{Ncat} > 1$ was instead found for 155 satellites, $R_{Ncat} > 2$ for 110, $R_{Ncat} > 3$ for 99, $R_{Ncat} > 4$ for 59, $R_{Ncat} > 5$ for 53, $R_{Ncat} > 10$ for 29, and $R_{Ncat} > 20$ for two operational spacecraft (Cosmos 2455 and 2502).

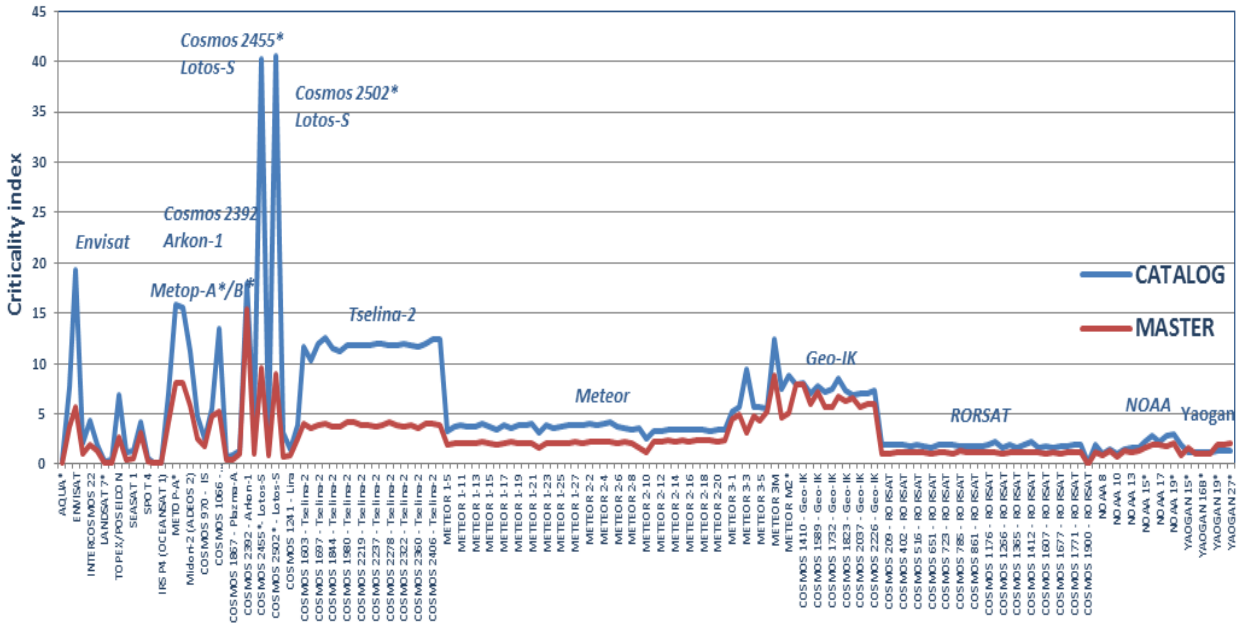

Fig. 13. Criticality index of the spacecraft in LEO with a perigee height ≥ 650 km and with a mass ≥ 1000 kg

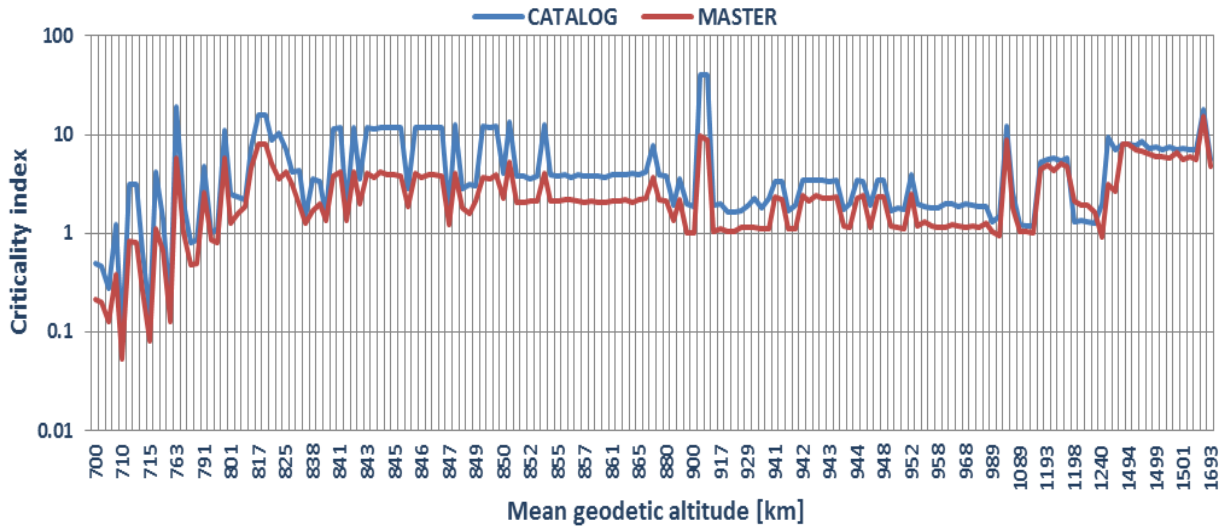

Fig. 14. Criticality index of the spacecraft in LEO with a perigee height ≥ 650 km and with a mass ≥ 1000 kg, as a function of the mean geodetic altitude

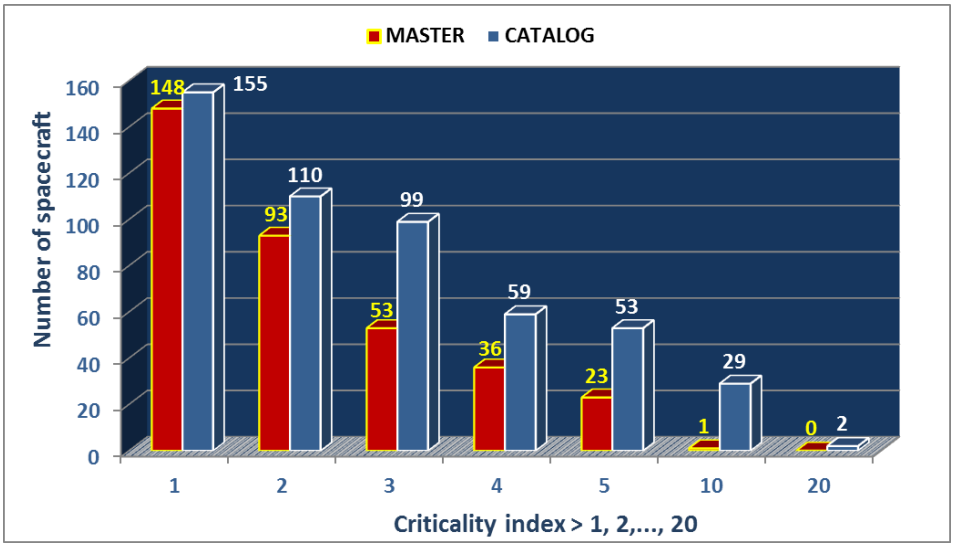

Fig. 15. Number of spacecraft having criticality indices, R_N & R_{Ncat}, larger than 1, 2, 3, 4, 5, 10 and 20

Concerning the further 737 constellation spacecraft with an individual mass < 1000 kg and a mean height > 900 km, the results obtained are summarized in Fig. 16. No R_N or $R_{Ncat} > 2$ was found. $R_N > 1$ was attained for 92 Parus, 24 Globalstar, 7 Tsiklon, 18 Tsikada, and 5 Sfera, i.e. 146 satellites in total, while $R_{Ncat} > 1$ was attained for 92 Parus, 11 Tsiklon, 18 Tsikada, and 7 Sfera, i.e. 128 satellites.

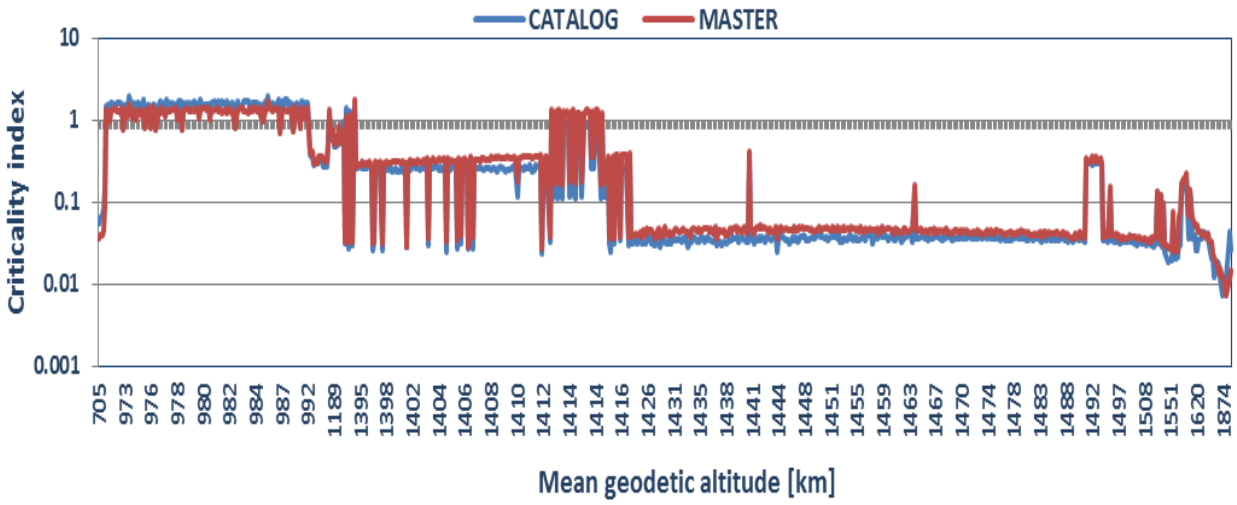

Fig. 16. Criticality index of the constellation satellites in LEO with an individual mass < 1000 kg and a mean height > 900 km, as a function of the mean geodetic altitude

6. Criticality of orbital stages

The values of R_N and R_{Ncat} obtained for the 434 orbital stages in LEO, with perigee height ≥ 650 km and mass ≥ 1000 kg, are summarized in Figs. 17-25. Again, R_N (MASTER) is always plotted in brown and R_{Ncat} (CATALOG) is always plotted in blue. For the only Japanese H-2A upper stage (M = 3000 kg, see Table B.3) present in the region of interest when the analysis was carried out (catalog number 27601), R_N = 2.23 and R_{Ncat} = 5.97. Tables B.1–B.9, in Appendix B, show the mean altitude, inclination and mass for each of the 434 orbital stages considered in this analysis.

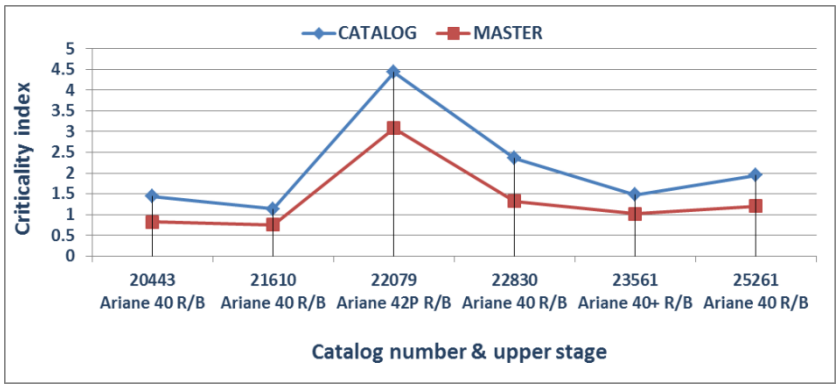

Fig. 17. Criticality index of the European Ariane 4 upper stages (1800 kg), Table B.1

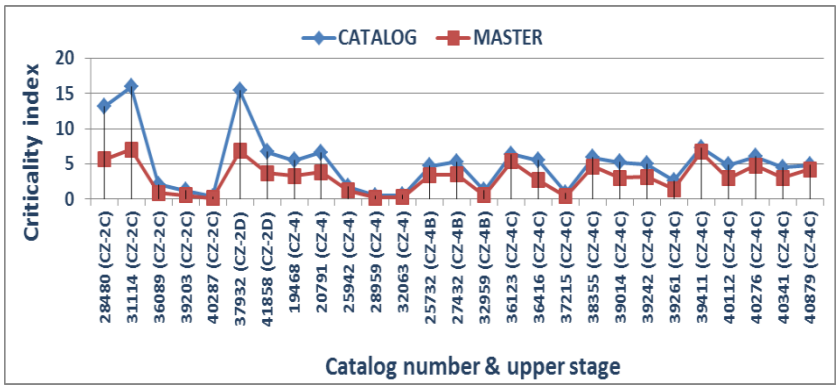

Fig. 18. Criticality index of the Chinese Long March upper stages ($M = 4000$ kg for CZ-2; $M = 2000$ kg for CZ-4), Table B.2

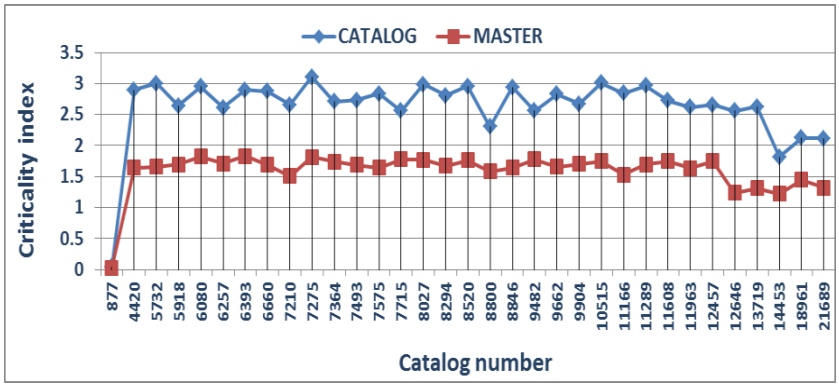

Fig. 19. Criticality index of the Russian SL-3 Vostok upper stages ($M = 1100$ kg), Table B.4

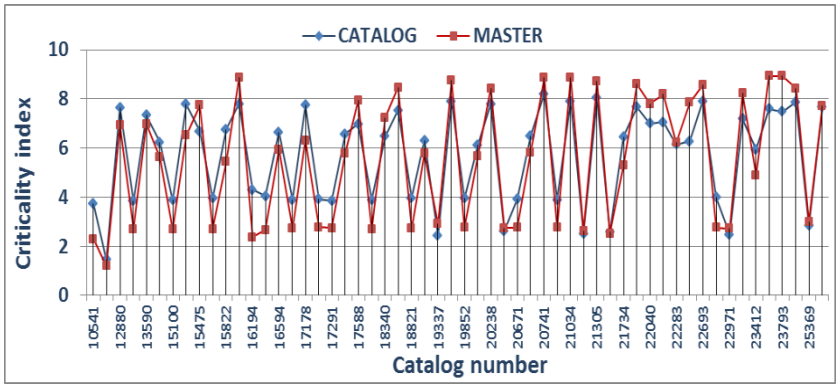

Fig. 20. Criticality index of the Ukrainian SL-14 Tsyklon-3 upper stages ($M = 1407$ kg), Table B.5

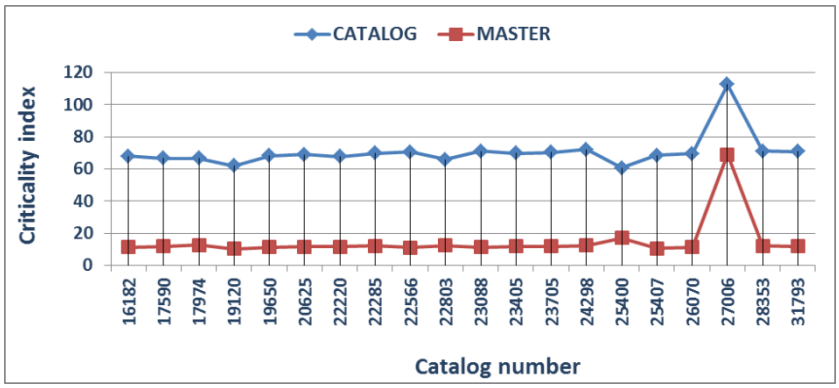

Fig. 21. Criticality index of the Russian SL-16 Zenit-2 upper stages ($M = 9000$ kg), Table B.6

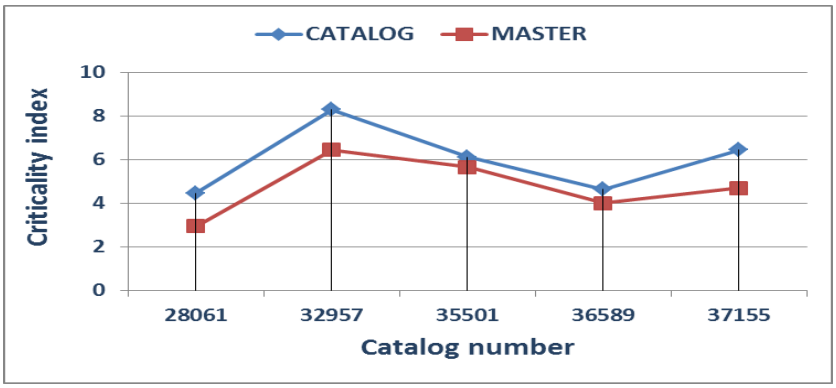

Fig. 22. Criticality index of the Russian SL-19 Rokot upper stages ($M = 1600$ kg), Table B.7

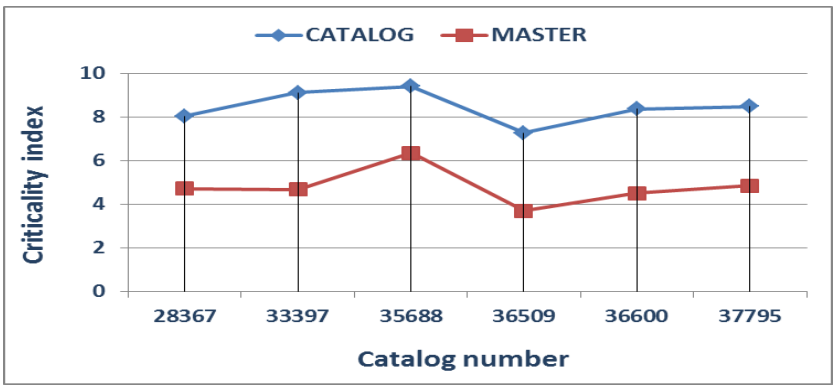

Fig. 23. Criticality index of the Ukrainian SL-24 Dnepr-1 upper stages ($M = 2360$ kg), Table B.8

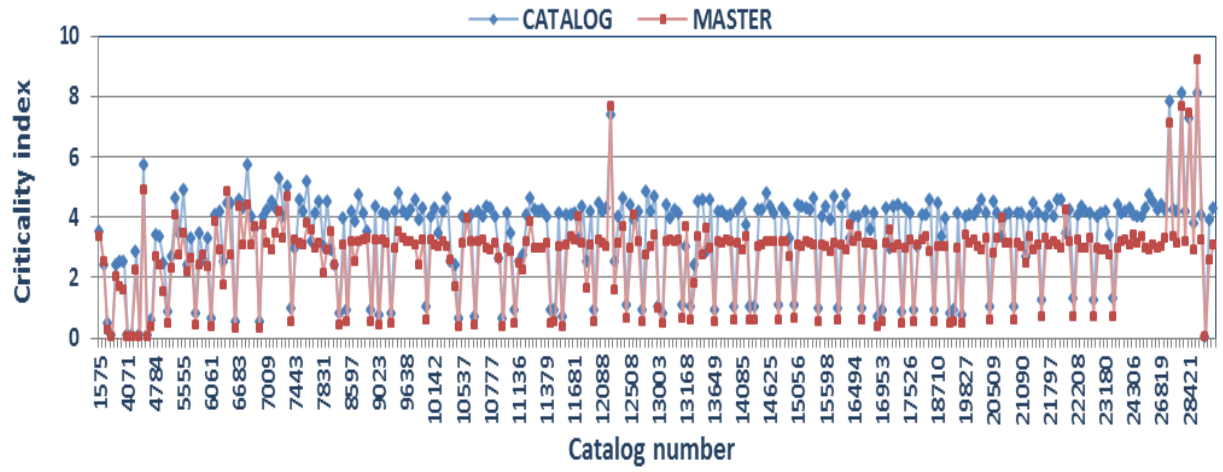

Fig. 24. Criticality index of the Russian SL-8 Kosmos upper stages (M = 1435 kg), Table B.9

Above 780 km, all the upper stages considered had both criticality indexes > 1 (Fig. 25). The most critical objects resulted to be the 20 SL-16 Zenit second stages (Fig. 21), with $R_N > 10$ and $R_{Ncat} > 60$.
As shown in Fig. 26, $R_N > 1$ was found for 367 abandoned rocket bodies, $R_N > 2$ for 320, $R_N > 3$ for 233, $R_N > 4$ for 86, $R_N > 5$ for 66, $R_N > 10$ for the 20 Zenit stages, and $R_N > 60$ for the Zenit stage with catalog number 27006. $R_{Ncat} > 1$ was instead found for 388 orbital stages, $R_{Ncat} > 2$ for 363, $R_{Ncat} > 3$ for 302, $R_{Ncat} > 4$ for 250, $R_{Ncat} > 5$ for 87, $R_{Ncat} > 10$ for 23, $R_{Ncat} > 20$ for the 20 Zenit stages, and $R_{Ncat} > 100$ for just one of these stages, again number 27006.

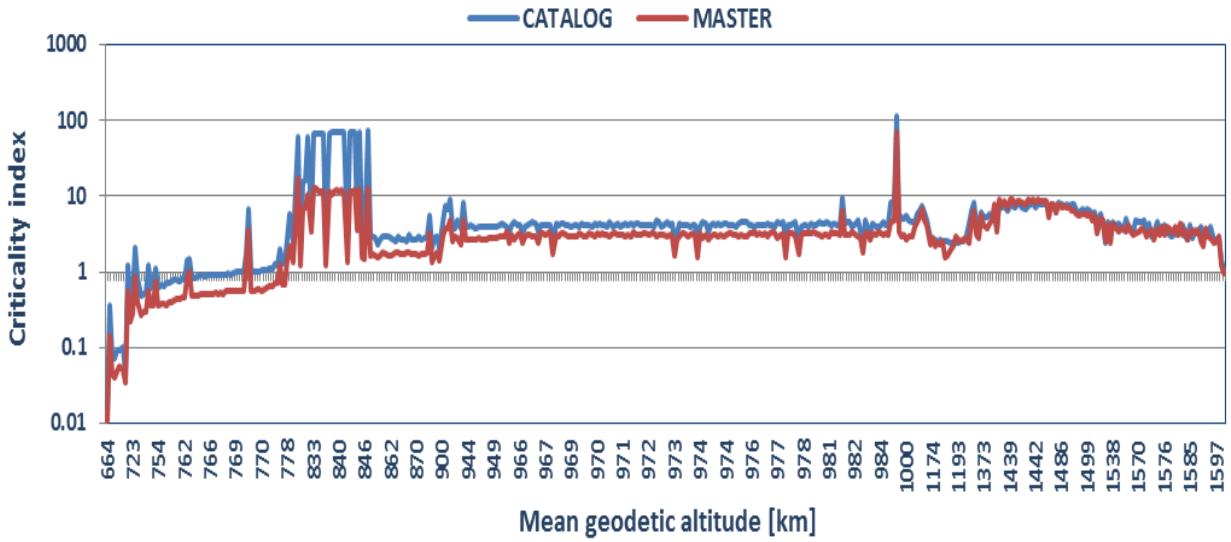

Fig. 25. Criticality index of the orbital stages in LEO with a perigee height ≥ 650 km and with a mass ≥ 1000 kg, as a function of the mean geodetic altitude

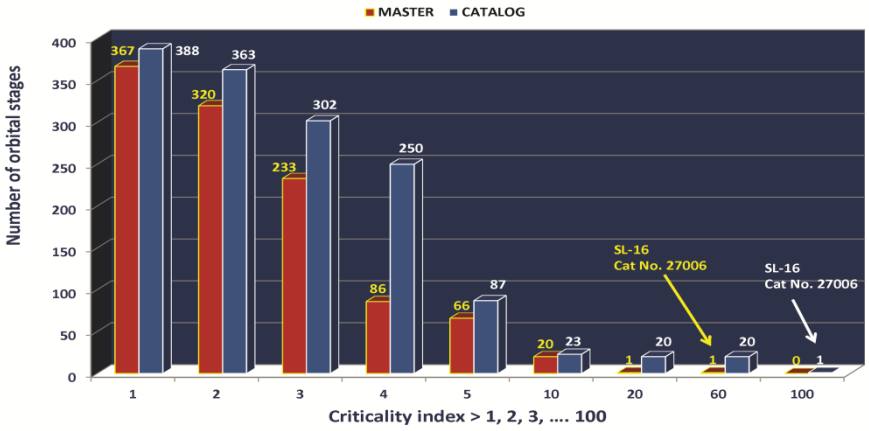

Fig. 26. Number of orbital stages having criticality indices, R_N & R_{Ncat}, larger than 1, 2, 3, 4, 5, 10, 20, 60 and 100

7. Remediation and mitigation applications

The assignment of a criticality index to the LEO intact objects is a first step to rank them as potential targets for active debris removal, if and when such remediation measure will become feasible. A higher criticality index will correspond to a higher removal priority, in terms of the expected long-term benefits for the debris environment.

As shown in the previous analysis and made clearer in Figs. 27-29, there would be plenty of targets for ADR: among the intact objects analyzed, 148 spacecraft with $M \geq 1000$ kg, 146 spacecraft with $M < 1000$ kg and 367 orbital stages with $M \geq 1000$ kg resulted to have $R_N > 1$, i.e. a potential debris environment criticality greater than that associated with a 1-ton object abandoned in sun-synchronous orbit at 800 km. And even though a few tens of the spacecraft were still operational when the analysis was carried out, the abandoned objects with $R_N > 1$ were more than 600.

The spacecraft with $M \geq 1000$ kg and $R_N > 1$ spanned the altitude range from 700 to 1700 km, but were mostly concentrated between 800 and 1000 km, near 1200 km and close to 1500 km (Fig. 27). The spacecraft with $M < 1000$ kg and $R_N > 1$ were instead largely found between 900 and 1000 km and around 1400 km (Fig. 28). Finally, the rocket bodies with $R_N > 1$ extended across the altitude range from 750 to 1700 km, with two main concentrations, between 750 and 1200 km, and between 1350 and 1600 km (Fig. 29).

In addition to the priority ranking of potential targets for active removal and debris remediation, the criticality index may also be used for mitigation, in particular to evaluate in advance, for instance during mission design, planning, or operation, the relative appropriateness of end-of-life disposal orbits, or the possible impact of failed disposal maneuvers. Let consider, as an example, six satellites in sun-synchronous orbit, operational when the analysis was carried out: Aqua, Landsat 8 and Terra, at 700 km, Metop A and B, at 817 km, and NOAA 19, at 849 km. According to the IADC mitigation guidelines, all these spacecraft would have to be disposed into a significantly lower orbit, at the end-of-life, in order to comply with the "25-year rule". However, for Aqua ($R_N = 0.21$), Landsat 8 ($R_N = 0.20$) and Terra ($R_N = 0.38$), a failure to do so, remaining in the operational orbit, would have been much less critical, from the debris environment point of view, than for NOAA 19 ($R_N = 2.10$) and, even more, for Metop A ($R_N = 8.11$) and Metop B ($R_N = 8.01$), see Fig. 30.

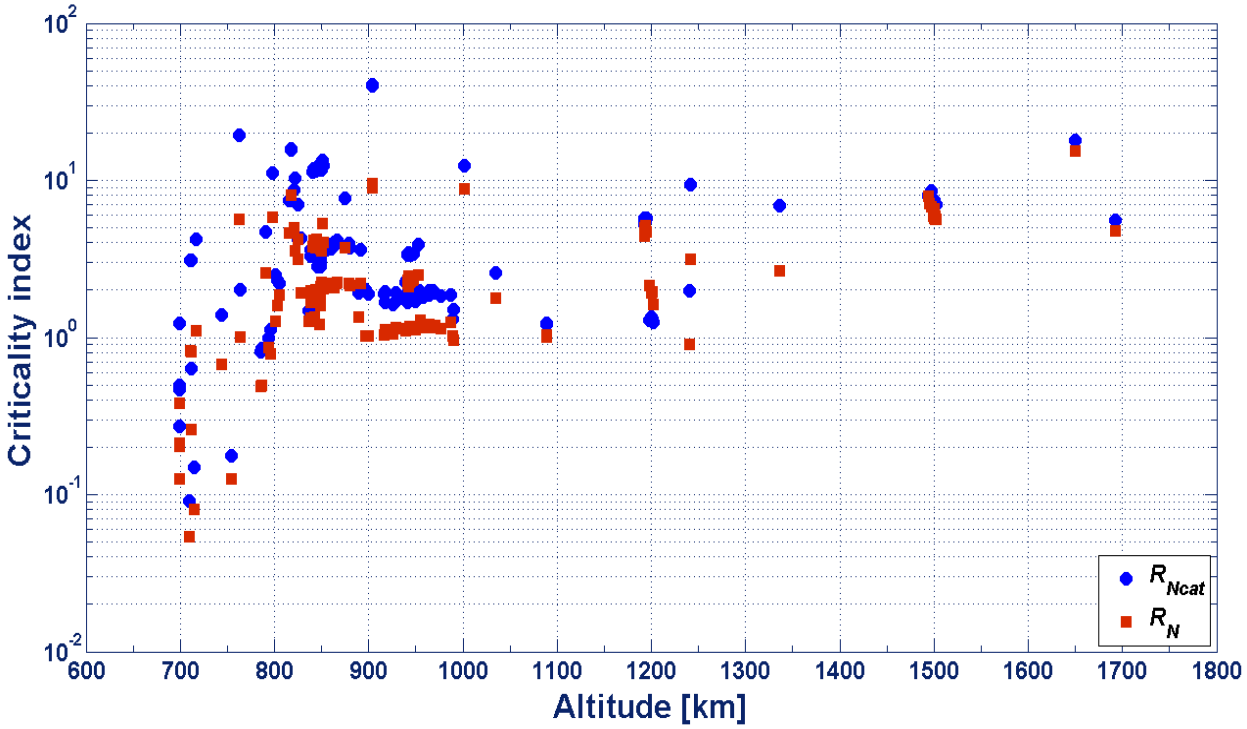

Fig. 27. Criticality index of the spacecraft in LEO with a perigee height ≥ 650 km and with a mass ≥ 1000 kg, as a function of the mean geodetic altitude

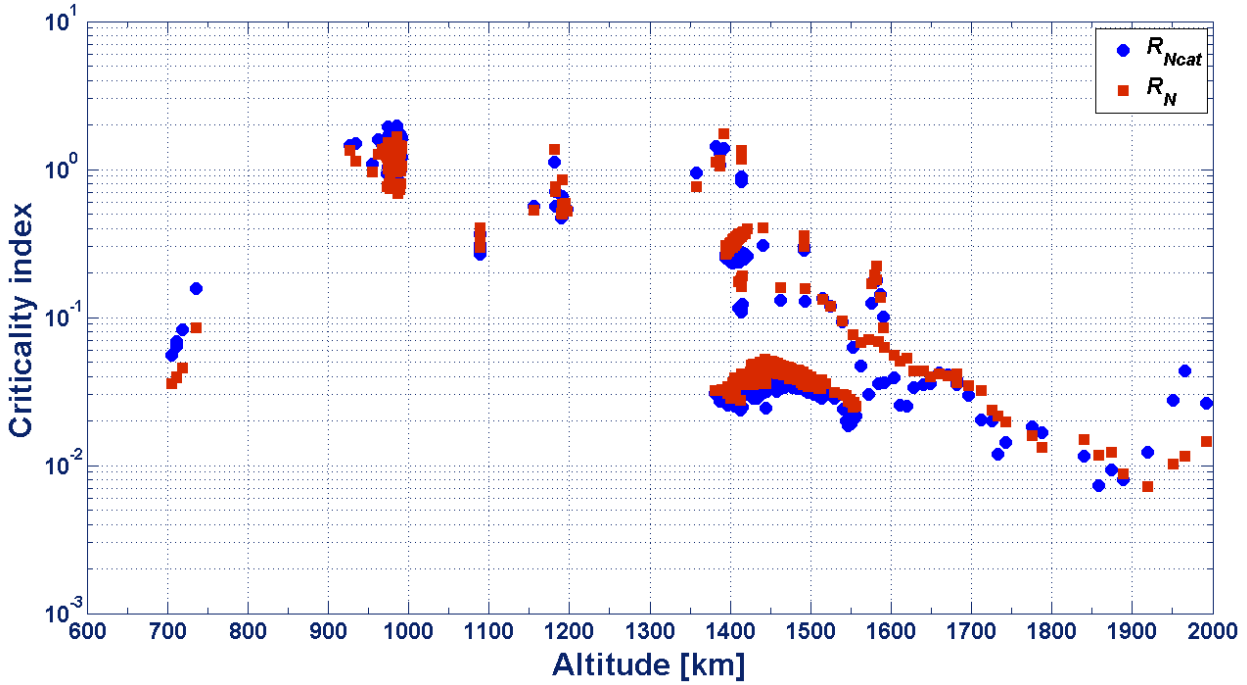

Fig. 28. Criticality index of the constellation satellites in LEO with an individual mass < 1000 kg and a mean height > 900 km, as a function of the mean geodetic altitude

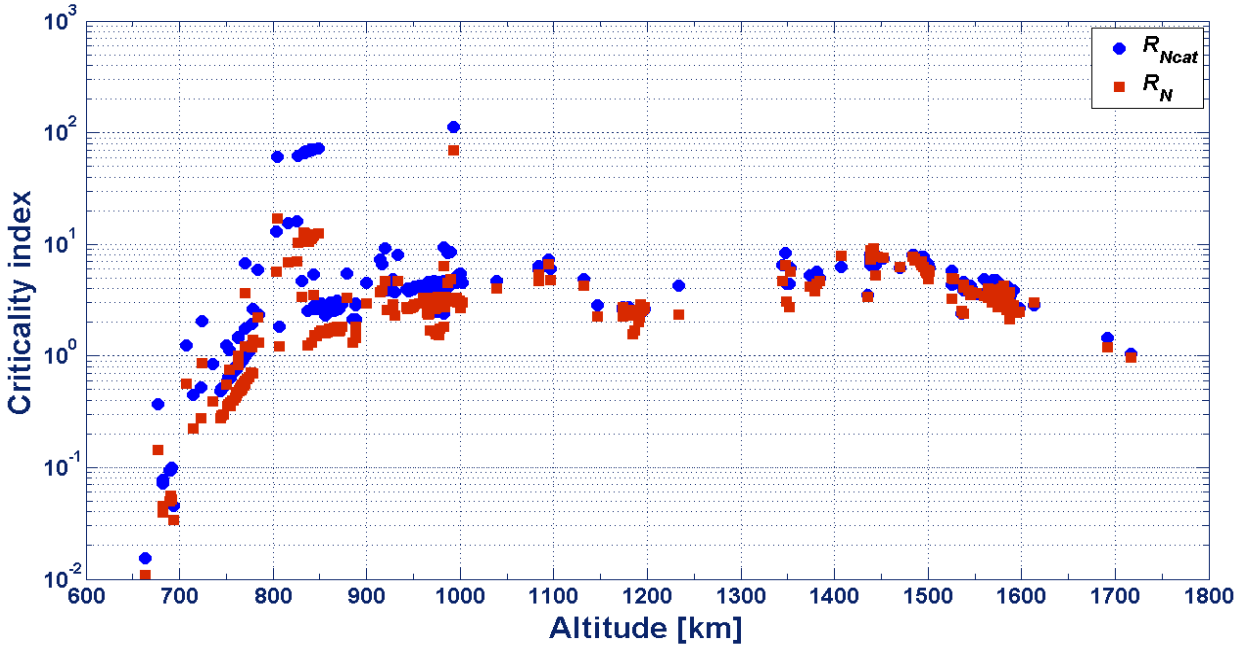

Fig. 29. Criticality index of the orbital stages in LEO with a perigee height ≥ 650 km and with a mass ≥ 1000 kg, as a function of the mean geodetic altitude

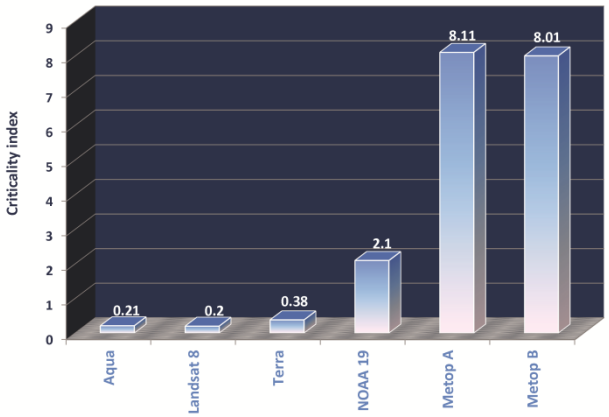

Fig. 30. Criticality index R_N for six satellites in sun-synchronous orbit, which were operational when the analysis was carried out (3 May 2017)

8. Conclusions

Among the 386 intact objects in LEO with $R_N > 2$, 83% were orbital stages and 17% spacecraft. Even considering the 116 objects with $R_N > 5$, the rocket bodies accounted for 80% of the total. This was certainly a good news from the debris remediation point of view, because the upper stages are probably an easier target for active removal, characterized as they are by a simpler shape, a high degree of geometric and mass distribution symmetry, a less fragile structure and, probably, a less complicated rotational

motion. In addition, they belong to a few families of similar objects, making the business of grappling and de-orbiting them repeatable many times with the same technologies and procedures.

There were 51 top ranking abandoned objects with $R_N > 7$, 46 (90%) orbital stages and 5 (10%) spacecraft. The latter are listed in Table 1. The European satellite Envisat, with $R_N = 5.69$, ranked 73rd, preceded by 59 orbital stages and 13 abandoned spacecraft. Regarding instead the top 46 rocket bodies, the situation is summarized in Table 2. The 20 SL-16 Zenit upper stages dominated the scene, between 800 and 1000 km, with the highest rankings associated with the two rocket bodies left in sun-synchronous orbit. Then followed 5 SL-8 Kosmos and 20 SL-14 Tsyklon-3 upper stages, between 1400 and 1500 km, and a single CZ-2C rocket body, abandoned in sun-synchronous orbit at 825 km.

Table 1. Abandoned satellites with $R_N > 7$ (3 May 2017)

Name	Mass [kg]	Height [km]	Inclination [deg]	R_N
Cosmos 2392†	6000	1649	63°	15.34
Meteor 3M	2500	1001	99°	8.80
Cosmos 1312††	1500	1494	83°	7.99
Cosmos 1410††	1500	1494	83°	7.95
Cosmos 1589††	1500	1495	83°	7.12

† Arkon-1 satellite

†† Geo-IK satellites

Table 2. Orbital stages with $R_N > 7$ (3 May 2017)

Type	Mass [kg]	Height [km]	Inclination [deg]	R_N
SL-16 stage Catalog #27006	9000	993	99°	69.07
SL-16 stage Catalog #25400	9000	804	98°	16.99
18 SL-16 stages	9000	≥ 826 ≤ 849	71°	10.29 12.66
4 SL-8 stages	1435	≥ 1441 ≤ 1486	82°	7.12 9.22
20 SL-14 stages	1407	~ 1440	83°	7.72 8.93
SL-8 stage Catalog #12115	1435	1453	74°	7.64
CZ-2C stage Catalog #31114	4000	825	98°	7.06

Concerning the R_{Ncat} index, much easier to be computed and updated, overall the ranking order was roughly the same obtained with R_N, but presented significant changes in the top list. There were 76 top ranking abandoned objects with $R_N \geq 7.6$, 46 (61%) orbital stages and 30 (39%) spacecraft. Among the abandoned spacecraft (see Fig. 31), Envisat became the leader, with $R_{Ncat} = 19.33$, followed by Cosmos 2392 (Arkon-1, $R_{Ncat} = 17.88$), Cosmos 1066 (Astrofizika, $R_{Ncat} = 13.41$), Meteor 3M ($R_{Ncat} = 12.36$), 19

Tselina-2 spacecraft ($10.33 \le R_{Ncat} \le 12.52$), Midori-2 ($R_{Ncat} = 11.21$), Meteor 3-3 ($R_{Ncat} = 9.42$), four Geo-IK geodesy satellites, Cosmos 1803 ($R_{Ncat} = 8.51$), 1410 ($R_{Ncat} = 8.08$), 1312 ($R_{Ncat} = 7.95$) and 1589 ($R_{Ncat} = 7.72$), and COBE ($R_{Ncat} = 7.68$).

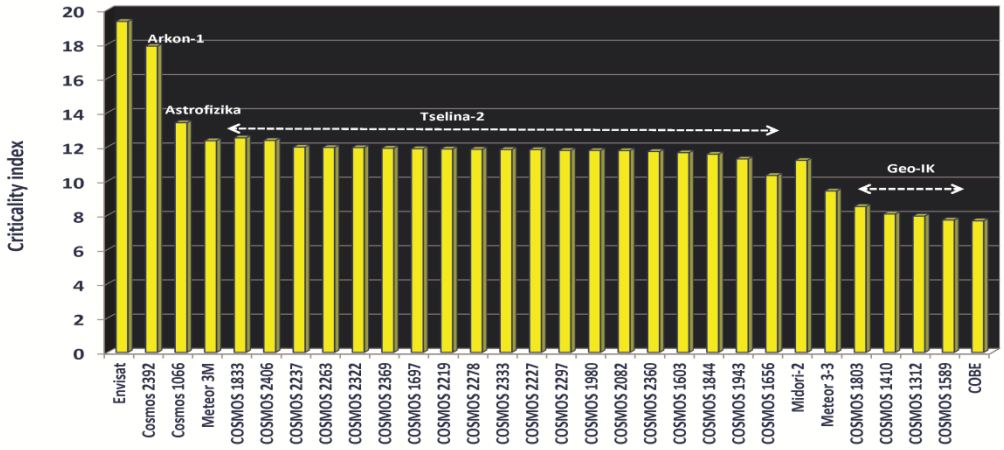

Fig. 31. Criticality index R_{Ncat} for abandoned spacecraft

Regarding the orbital stages (Fig. 32), the ranking list was much more stable. Looking again at the top 46 rocket bodies, the leader was again the SL-16 Zenit upper stage with catalog number 27006 ($R_{Ncat} = 112.50$), followed by the other 19 twin stages ($60.71 \le R_{Ncat} \le 79.09$). The list continued with one CZ-2D and two CZ-2C rocket bodies ($13.14 \le R_{Ncat} \le 15.98$), five SL-24 Dnepr-1 upper stages ($8.05 \le R_{Ncat} \le 9.41$), one SL-19 Rokot upper stage ($R_{Ncat} = 8.30$), 14 SL-14 Tsyklon-3 upper stages ($7.60 \le R_{Ncat} \le 8.20$), and three SL-8 Kosmos stages ($7.84 \le R_{Ncat} \le 8.12$), see Fig. 32.

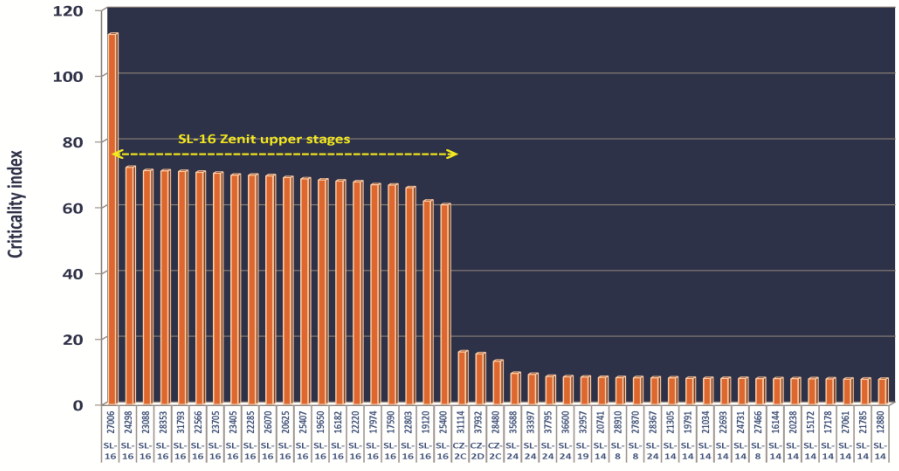

Fig. 32. Criticality index R_{Ncat} for orbital stages

In conclusion, the environmental criticality of the main intact objects abandoned in LEO, both spacecraft and orbital stages, was coherently estimated with a couple of new criticality indexes. The results obtained identified and ranked several hundreds of suitable targets for active debris removal, if such remediation measure will become economically feasible on a large scale in the future. However, the criticality indexes detailed in the paper might also be used for mitigation purposes, in particular during mission design and planning, for instance to assess the relative merits and drawbacks of operational and disposal orbits, both for spacecraft and upper stages, from the debris environment point of view.

Acknowledgements

The authors thank the US Space Track Organization (www.space-track.org) for making available the catalog of the unclassified objects tracked around the Earth by the US Space Surveillance Network, and the European Space Agency (ESA) for the MASTER-2009 population of objects larger than 10 cm.

Concerning the data on spacecraft and orbital stages, particularly the mass, the authors are indebted to the European Space Agency (ESA) DISCOS Database (discosweb.esoc.esa.int), to the Mark Wade's Encyclo-pedia Astronautica (www.astronautix.com), to the NASA Space Science Data Coordinated Archive (nssdc.gsfc.nasa.gov), and to the IHS Jane's Space Systems & Industry 2012-2013 book.

Regarding the operational status of the satellites, special thanks go to the Union of Concerned Scientists (UCS) Satellite Database (www.ucsusa.org/nuclear-weapons/space-weapons/satellite-database).

References

[1] D.J. Kessler, B.G. Cour-Palais, Collision frequency of artificial satellites: the creation of a debris belt, J. Geophys. Res. 83 (1978) 2637–2646.

[2] Scientific and Technical Subcommittee, Technical Report on Space Debris, Committee on the Peaceful Uses of Outer Space, United Nations, New York, 1999.

[3] Steering Group & Working Group 4, Space Debris Mitigation Guidelines, Document IADC-02-01 (2002) & Revision 1 (2007), Inter-Agency Space Debris Coordination Committee (IADC).

[4] L. Anselmo, The long-term evolution of the space debris environment, Proc. 3rd European Conference on Space Debris, ESA SP-473, Vol. 1, European Space Agency, Noordwijk (NL), 2001, pp. 333–340.

[5] L. Anselmo, A. Rossi, C. Pardini, A. Cordelli, R. Jehn, Effect of mitigation measures on the long-term evolution of the debris population, Adv. Space Res. 28 (2001) 1427–1436.

[6] NASA Orbital Debris Program Office, Monthly mass of objects in Earth orbit by object type, Orbital Debris Quarterly News 21-1 (2017) 13.

[7] D.S. McKnight, Engineering and operational issues related to just-in-time collision avoidance (JCA), FP-EUCASS-266, 6th European Conference for Aeronautics and Space Sciences (EUCASS), Krakow, Poland, 29 June – 3 July 2015.

[8] J.C. Dolado-Perez, C. Pardini, L. Anselmo, Review of uncertainty sources affecting the long-term predictions of space debris evolutionary models, Acta Astronaut. 113 (2015) 51–65.

[9] J.C. Liou, N.L. Johnson, A sensitivity study of the effectiveness of active debris removal in LEO, Acta Astronaut. 64 (2009) 236–243.

[10] J.C. Liou, An active debris removal parametric study for LEO environment remediation, Adv. Space Res. 47 (2011) 1865–1876.

[11] J. Utzmann, M. Oswald, S. Stabroth, P. Voigt, A. Wagner, I. Retat, Ranking and characterization of heavy debris for active removal, IAC-12-A6.2.8, 63rd International Astronautical Congress, Naples, Italy, 1 – 5 October 2012.

[12] L.T. DeLuca, M. Lavagna, F. Maggi, P. Tadini, C. Pardini, L. Anselmo, M. Grassi, U. Tancredi, A. Francesconi, S. Chiesa, N. Viola, V. Trushlyakov, Active removal of large massive objects by hybrid propulsion module, Proc. 5th European Conference for Aero-Space Sciences, EUCASS, 2013, Paper p469.
[13] J. Radtke, S.K. Flegel, S. Roth, H. Krag, Deriving the spacecraft environment criticality from Monte-Carlo simulations of the space debris environment, IAC-14-A6.2.6, 65th International Astronautical Congress, Toronto, Canada, 29 September – 3 October 2014.
[14] A. Rossi, G.B. Valsecchi, E.M. Alessi, An evaluation index for the ranking of LEO objects, IAC-14-A6.2.7, 65th International Astronautical Congress, Toronto, Canada, 29 September – 3 October 2014.
[15] A. Rossi, G.B. Valsecchi, E.M. Alessi, The criticality of spacecraft index, Adv. Space Res. 56 (2015) 449–460.
[16] F. Letizia, C. Colombo, H.G. Lewis, H. Krag, Extending the ECOB space debris index with fragmentation risk estimation, Proc. 7th European Conference on Space Debris, ESA/ESOC, Darmstadt, Germany, 2017, SDC7-paper417.
[17] C. Colombo, F. Letizia, M. Trisolini, H.G. Lewis, A. Chanoine, P.-A. Duvernois, J. Austin, S. Lemmens, Life cycle assessment indicator for space debris, Proc. 7th European Conference on Space Debris, ESA/ESOC, Darmstadt, Germany, 2017, SDC7-paper822.
[18] L. Anselmo, C. Pardini, Compliance of the Italian satellites in low Earth orbit with the end-of-life disposal guidelines for space debris mitigation, IAC-14-A6.4.5, 65th International Astronautical Congress, Toronto, Canada, 29 September – 3 October 2014.
[19] L. Anselmo, C. Pardini, Compliance of the Italian satellites in low Earth orbit with the end-of-life disposal guidelines for space debris mitigation and ranking of their long-term criticality for the environment, Acta Astronaut. 114 (2015) 93–100.
[20] L. Anselmo, C. Pardini, An index for ranking active debris removal targets in LEO, Proc. 7th European Conference on Space Debris, ESA/ESOC, Darmstadt, Germany, 2017, SDC7-paper152.
[21] L. Anselmo, C. Pardini, Ranking upper stages in low Earth orbit for active removal, Acta Astronaut. 122 (2016) 19–27.
[22] C. Pardini, L. Anselmo, Characterization of aban-doned rocket body families for active removal. Acta Astronaut. 126 (2016) 243–257.
[23] NASA Orbital Debris Program Office, Monthly effective mass of objects in Earth orbit by region, Orbital Debris Quarterly News 19-1 (2015) 9.
[24] C. Pardini, L. Anselmo, Review of past on-orbit collisions among cataloged objects and examination of the catastrophic fragmentation concept, Acta Astronaut. 100 (2014) 30–39.
[25] N.L. Johnson, P.H. Krisko, J.-C. Liou, P.D. Anz-Meador, NASA's new breakup model of EVOLVE 4.0, Adv. Space Res. 28 (2001) 1377–1384.
[26] P.H. Krisko, Proper implementation of the 1998 NASA breakup model, Orbital Debris Quarterly News 15-4 (2011) 4–5.
[27] C. Pardini, L. Anselmo, Physical properties and long-term evolution of the debris clouds produced by two catastrophic collisions in Earth orbit, Adv. Space Res. 48 (2011) 557–569.
[28] A. Rossi, P. Farinella, Collision rates and impact velocities for bodies in low earth orbit, ESA J. 16 (1992) 339–348.
[29] C. Pardini, L. Anselmo, Assessing the risk of orbital debris impact, Space Debris 1 (1999) 59–80.
[30] D.S. McKnight, Collision and breakup models: pedigree, regimes, and validation/verification, Briefing presented to the National Research Council Committee on Space Debris Workshop, Irvine, California, 1993.
[31] Meteoroid and Space Debris Terrestrial Environment Reference (MASTER-2009), ESA-SD-DVD-02, Release 1.0, Institute of Aerospace Systems, Technical University of Braunschweig, Germany, December 2010.
[32] C. Pardini, L. Anselmo, SDIRAT: introducing a new method for orbital debris collision risk assessment, Paper MS00/23, 15th International Symposium on Space Flight Dynamics, Biarritz, France, 26 – 30 June 2000.

Appendix A

Table A.1. 12 Russian Geo-IK geodesy satellites (3 May 2017)

Satellite name	USSTRATCOM catalog number	Mean altitude [km]	Inclination [deg]	Mass [kg]
COSMOS 1312	12879	1494.04	82.60	1500.00
COSMOS 1410	13589	1494.17	82.61	1500.00
COSMOS 1510	14521	1499.59	73.62	1500.00
COSMOS 1589	15171	1494.64	82.60	1500.00
COSMOS 1660	15821	1501.27	73.62	1500.00
COSMOS 1732	16593	1500.17	73.61	1500.00
COSMOS 1803	17177	1497.34	82.61	1500.00
COSMOS 1823	17535	1498.86	73.60	1500.00
COSMOS 1950	19195	1500.68	73.60	1500.00
COSMOS 2037	20196	1501.92	73.56	1500.00
COSMOS 2088	20720	1501.41	73.60	1500.00
COSMOS 2226	22282	1499.26	73.62	1500.00

Table A.2. 14 Heterogeneous Cosmos satellites, with mass up to 7000 kg (3 May 2017)

Satellite name	USSTRATCOM catalog number	Mean altitude [km]	Inclination [deg]	Mass [kg]
COSMOS 2502* – Lotos-S	40358	903.66	67.15	7000.00
COSMOS 2455* – Lotos-S	36095	903.44	67.15	7000.00
COSMOS 2441 – Persona	33272	717.14	97.94	7000.00
COSMOS 2486* – Persona	39177	711.03	98.14	6500.00
COSMOS 2506* – Persona	40699	711.38	98.20	6500.00
COSMOS 2392 – Arkon-1	27470	1649.41	63.43	6000.00
COSMOS 1045 – Meteor-2	11084	1692.81	82.54	3369.67
COSMOS 1066 – Astrofizika	11165	851.24	81.24	2725.47
COSMOS 1375 – Lira	13259	952.29	65.83	1982.16
COSMOS 970 - IS	10531	1034.84	65.85	1486.62
COSMOS 1818 – Plazma-A	17369	785.59	65.01	1250.00
COSMOS 1867 – Plazma-A	18187	786.64	65.01	1250.00
COSMOS 1241 – Lira	12149	990.33	65.83	1045.00
COSMOS 2285 – Obzor	23189	989.16	74.03	817.64

Table A.3. 20 Heterogeneous satellites from Europe, United States and Japan (3 May 2017)

Satellite name	USSTRATCOM catalog number	Mean altitude [km]	Inclination [deg]	Mass [kg]
ENVISAT	27386	762.58	98.23	8110.00
TERRA*	25994	699.57	98.21	4854.00
METOP-A*	29499	817.40	98.68	4086.00
METOP-B*	38771	817.50	98.68	4086.00
Midori-2 (ADEOS 2)	27597	797.95	98.37	3680.00
AQUA*	27424	699.57	98.20	2832.00
LANDSAT 8*	39084	699.57	98.23	2782.00
SPOT 4	25260	711.44	98.35	2600.00
ARGOS	25634	824.80	98.62	2490.00
Midori (ADEOS 1)	24277	790.92	98.72	2468.78
TOPEX/POSEIDON	22076	1335.99	66.04	2402.00
SEASAT 1	10967	744.32	108.01	2279.48
COBE	20322	874.45	98.95	2265.00
ERS 1	21574	763.73	98.46	2140.73
LANDSAT 7*	25682	699.57	98.22	2020.00
SPOT 3	22823	825.31	98.94	1890.98
INTERCOSMOS 22	12645	828.30	81.22	1486.62
FUSE-1	25791	753.97	24.98	1130.00
IRAS	13777	889.70	98.96	1063.43
IRS P4 (OCEANSAT 1)	25758	715.04	98.16	1050.00

Table A.4. 11 NOAA meteorological satellites (3 May 2017)

Satellite name	USSTRATCOM catalog number	Mean altitude [km]	Inclination [deg]	Mass [kg]
NOAA 8	13923	793.55	98.51	1004.96
NOAA 9	15427	836.17	98.80	1004.96
NOAA 10	16969	795.54	98.46	1004.96
NOAA 11	19531	838.85	98.56	1004.96
NOAA 13	22739	847.40	98.57	1020.81
NOAA 14	23455	842.65	98.69	1060.46
NOAA 15*	25338	803.07	98.78	1441.03
NOAA 16	26536	845.73	98.86	1403.00
NOAA 17	27453	805.65	98.43	1403.00
NOAA 18*	28654	848.62	99.18	1420.00
NOAA 19*	33591	849.09	99.09	1420.00

Table A.5. 20 Russian Tselina-2 electronic intelligence satellites (3 May 2017)

Satellite name	USSTRATCOM catalog number	Mean altitude [km]	Inclination [deg]	Mass [kg]
COSMOS 1603	15333	843.39	71.03	3221.01
COSMOS 1656	15755	821.97	71.11	3221.01
COSMOS 1697	16181	845.72	70.96	3221.01
COSMOS 1833	17589	847.46	70.92	3221.01
COSMOS 1844	17973	843.56	70.90	3221.01
COSMOS 1943	19119	840.01	71.01	3221.01
COSMOS 1980	19649	841.34	71.00	3221.01
COSMOS 2082	20624	842.78	71.04	3221.01
COSMOS 2219	22219	844.94	71.06	3221.01
COSMOS 2227	22284	846.00	70.98	3221.01
COSMOS 2237	22565	849.14	70.83	3221.01
COSMOS 2263	22802	846.50	70.93	3221.01
COSMOS 2278	23087	844.41	71.05	3221.01
COSMOS 2297	23404	845.37	71.01	3221.01
COSMOS 2322	23704	845.89	70.98	3221.01
COSMOS 2333	24297	846.14	70.90	3221.01
COSMOS 2360	25406	849.51	70.81	3171.46
COSMOS 2369	26069	845.77	71.00	3200.00
COSMOS 2406	28352	851.72	71.01	3200.00
COSMOS 2428*	31792	849.54	70.91	3250.00

Table A.6. 31 Russian US-A radar ocean reconnaissance satellites (RORSAT), 3 May 2017

Satellite name	USSTRATCOM catalog number	Mean altitude [km]	Inclination [deg]	Mass [kg]
COSMOS 198	3081	915.92	65.14	1250.00
COSMOS 209	3158	900.17	65.33	1250.00
COSMOS 367	4564	967.96	65.28	1250.00
COSMOS 402	5105	987.10	64.98	1250.00
COSMOS 469	5721	976.81	64.49	1250.00
COSMOS 516	6154	970.84	64.81	1250.00
COSMOS 626	7005	943.53	65.44	1250.00
COSMOS 651	7291	917.01	64.97	1250.00
COSMOS 654	7297	964.44	64.95	1250.00
COSMOS 723	7718	929.16	64.72	1250.00
COSMOS 724	7727	896.25	65.59	1250.00
COSMOS 785	8473	954.58	65.07	1250.00
COSMOS 860	9486	957.95	65.00	1250.00
COSMOS 861	9494	957.01	64.86	1250.00
COSMOS 952	10358	949.79	64.93	1250.00
COSMOS 1176	11788	916.94	64.83	1250.00
COSMOS 1249	12319	939.03	64.96	1250.00
COSMOS 1266	12409	925.85	64.76	1250.00

COSMOS 1299	12783	943.58	65.12	1250.00
COSMOS 1365	13175	928.71	65.07	1250.00
COSMOS 1372	13243	941.49	64.90	1250.00
COSMOS 1412	13600	940.43	64.81	1250.00
COSMOS 1579	15085	941.27	65.05	1250.00
COSMOS 1607	15378	949.97	65.00	1250.00
COSMOS 1670	15930	949.36	64.94	1250.00
COSMOS 1677	15986	939.44	64.68	1250.00
COSMOS 1736	16647	964.58	64.99	1250.00
COSMOS 1771	16917	953.68	64.98	1250.00
COSMOS 1860	18122	945.53	65.01	1250.00
COSMOS 1900	18665	709.56	66.08	1250.00
COSMOS 1932	18957	963.74	65.05	1250.00

Table A.7. 8 Chinese Yaogan reconnaissance satellites (3 May 2017)

Satellite name	USSTRATCOM catalog number	Mean altitude [km]	Inclination [deg]	Mass [kg]
YAOGAN 8*	36121	1240.34	100.08	1040.00
YAOGAN 15*	38354	1202.16	100.37	1040.00
YAOGAN 16A*	39011	1088.86	63.38	1040.00
YAOGAN 16B*	39012	1088.86	63.38	1040.00
YAOGAN 16C*	39013	1088.89	63.38	1040.00
YAOGAN 19*	39410	1201.43	100.33	1040.00
YAOGAN 22*	40275	1200.00	100.40	1040.00
YAOGAN 8*	36121	1240.34	100.08	1040.00

Table A.8. 49 Russian Meteor meteorological satellites, with mass up to 2900 kg (Meteor M2), 3 May 2017

Satellite name	USSTRATCOM catalog number	Mean altitude [km]	Inclination [deg]	Mass [kg]
METEOR 1-5	4419	838.34	81.21	1280.00
METEOR 1-10	5731	851.60	81.26	1280.00
METEOR 1-11	5917	861.19	81.22	1280.00
METEOR 1-12	6079	880.31	81.22	1280.00
METEOR 1-13	6256	860.53	81.27	1280.00
METEOR 1-14	6392	865.04	81.24	1280.00
METEOR 1-15	6659	857.11	81.19	1280.00
METEOR 1-16	7209	843.33	81.23	1280.00
METEOR 1-17	7274	861.88	81.24	1280.00
METEOR 1-18	7363	891.52	81.22	1280.00
METEOR 1-19	7490	856.55	81.18	1280.00
METEOR 1-20	7574	851.71	81.23	1280.00
METEOR 1-21	7714	863.58	81.21	1280.00
METEOR 1-22	8293	848.93	81.26	1280.00
METEOR 1-23	8519	853.97	81.24	1280.00
METEOR 1-24	8799	851.67	81.26	1280.00
METEOR 1-25	8845	851.50	81.26	1280.00
METEOR 1-26	9481	857.53	81.22	1280.00
METEOR 1-27	9903	862.64	81.24	1280.00
METEOR 2-1	8026	855.61	81.28	1300.00
METEOR 2-2	9661	878.79	81.27	1300.00
METEOR 2-3	10514	855.31	81.21	1300.00
METEOR 2-4	11288	850.38	81.22	1300.00
METEOR 2-5	11605	866.76	81.21	1300.00
METEOR 2-6	11962	854.66	81.22	1300.00
METEOR 2-7	12456	855.54	81.27	1300.00
METEOR 2-8	13113	942.11	82.54	1300.00
METEOR 2-9	13718	838.06	81.25	1300.00
METEOR 2-10	14452	800.86	81.16	1300.00
METEOR 2-11	15099	943.31	82.53	1300.00
METEOR 2-12	15516	941.18	82.53	1300.00
METEOR 2-13	16408	942.30	82.54	1300.00

METEOR 2-14	16735	942.37	82.54	1300.00
METEOR 2-15	17290	943.34	82.47	1300.00
METEOR 2-16	18312	944.40	82.56	1300.00
METEOR 2-17	18820	941.93	82.54	1300.00
METEOR 2-18	19851	940.98	82.52	1300.00
METEOR 2-19	20670	944.51	82.55	1300.00
METEOR 2-20	20826	946.02	82.52	1300.00
METEOR 2-21	22782	947.58	82.55	1300.00
METEOR 3-1	16191	1192.60	82.55	2215.00
METEOR 3-2	19336	1192.65	82.54	2215.00
METEOR 3-3	20305	1241.34	82.55	2215.00
METEOR 3-4	21232	1194.91	82.55	2215.00
METEOR 3-5	21655	1193.07	82.55	2215.00
METEOR 3-6	22969	1193.56	82.56	2215.00
METEOR 3M	27001	1001.13	99.40	2500.00
METEOR-M	35865	815.44	98.42	2700.00
METEOR M2*	40069	820.35	98.66	2900.00

Appendix B

Table B.1. 6 European Ariane 4 upper stages (3 May 2017)

Orbital stage of the launcher	USSTRATCOM catalog number	Mean altitude [km]	Inclination [deg]	Mass [kg]
Ariane 40 R/B	20443	762.40	98.73	1800.00
Ariane 40 R/B	21610	752.92	98.61	1800.00
Ariane 42P /B	22079	1348.76	66.07	1800.00
Ariane 40 R/B	22830	784.21	98.88	1800.00
Ariane 40+R/B	23561	763.01	98.79	1800.00
Ariane 40 R/B	25261	776.95	98.54	1800.00

Table B.2. 27 Chinese Long March upper stages (3 May 2017)

Orbital stage of the launcher	USSTRATCOM catalog number	Mean altitude [km]	Inclination [deg]	Mass [kg]
CZ-2C	28480	803.52	98.19	4000.00
CZ-2C	31114	824.95	98.41	4000.00
CZ-2C	36089	723.97	98.05	4000.00
CZ-2C	39203	707.47	98.34	4000.00
CZ-2C	40287	676.50	98.00	4000.00
CZ-2D	37932	816.03	98.53	4000.00
CZ-2D	41858	769.65	98.37	4000.00
CZ-4	19468	878.96	99.17	2000.00
CZ-4	20791	916.55	98.96	2000.00
CZ-4	25942	769.51	98.60	2000.00
CZ-4	28059	714.71	98.57	2000.00
CZ-4	32063	722.60	98.03	2000.00
CZ-4B	25732	830.55	98.99	2000.00
CZ-4B	27432	842.79	98.98	2000.00
CZ-4B	32959	750.25	98.87	2000.00
CZ-4C	36123	1084.25	100.51	2000.00
CZ-4C	36416	999.70	63.44	2000.00
CZ-4C	37215	735.54	98.76	2000.00
CZ-4C	38355	1083.85	100.26	2000.00
CZ-4C	39014	997.54	63.43	2000.00
CZ-4C	39242	998.90	63.46	2000.00
CZ-4C	39261	778.50	98.78	2000.00
CZ-4C	39411	1093.89	100.43	2000.00
CZ-4C	40112	1000.37	63.45	2000.00
CZ-4C	40276	1096.08	100.40	2000.00
CZ-4C	40341	1001.91	63.46	2000.00
CZ-4C	40879	1131.97	100.34	2000.00

Table B.3. 1 Japanese H2-A upper stage (3 May 2017)

Orbital stage of the launcher	USSTRATCOM catalog number	Mean altitude [km]	Inclination [deg]	Mass [kg]
H2-A	27601	783.165	98.381	3000

Table B.4. 33 Russian SL-3 Vostok upper stages (3 May 2017)

Orbital stage of the launcher	USSTRATCOM catalog number	Mean altitude [km]	Inclination [deg]	Mass [kg]
SL-3	877	694.10	65.08	1100.00
SL-3	4420	849.63	81.23	1100.00
SL-3	5732	870.58	81.25	1100.00
SL-3	5918	870.90	81.24	1100.00
SL-3	6080	888.07	81.24	1100.00
SL-3	6257	868.91	81.26	1100.00
SL-3	6393	873.77	81.26	1100.00
SL-3	6660	870.99	81.23	1100.00
SL-3	7210	846.30	81.24	1100.00
SL-3	7275	868.21	81.25	1100.00
SL-3	7364	870.35	81.24	1100.00
SL-3	7493	864.72	81.18	1100.00
SL-3	7575	853.15	81.25	1100.00
SL-3	7715	867.83	81.22	1100.00
SL-3	8027	865.72	81.30	1100.00
SL-3	8294	861.56	81.21	1100.00
SL-3	8520	860.26	81.29	1100.00
SL-3	8800	856.24	81.25	1100.00
SL-3	8846	861.48	81.23	1100.00
SL-3	9482	864.89	81.27	1100.00
SL-3	9662	887.77	81.27	1100.00
SL-3	9904	867.33	81.26	1100.00
SL-3	10515	861.08	81.24	1100.00
SL-3	11166	843.96	81.24	1100.00
SL-3	11289	851.29	81.25	1100.00
SL-3	11608	869.84	81.21	1100.00
SL-3	11963	857.85	81.28	1100.00
SL-3	12457	866.13	81.28	1100.00
SL-3	12646	836.73	81.22	1100.00
SL-3	13719	840.90	81.26	1100.00
SL-3	14453	806.89	81.17	1100.00
SL-3	18961	888.60	99.33	1100.00
SL-3	21689	884.72	99.31	1100.00

Table B.5. 56 Ukrainian SL-14 Tsyklon-3 upper stages (3 May 2017)

Orbital stage of the launcher	USSTRATCOM catalog number	Mean altitude [km]	Inclination [deg]	Mass [kg]
Sl-14	10541	929.979	75.835	1407.00
Sl-14	11087	1691.551	82.542	1407.00
Sl-14	12880	1491.907	82.598	1407.00
Sl-14	13114	944.617	82.543	1407.00
Sl-14	13590	1492.646	82.609	1407.00
Sl-14	14522	1497.835	73.618	1407.00
Sl-14	15100	945.352	82.534	1407.00
Sl-14	15172	1493.01	82.604	1407.00
Sl-14	15475	1440.384	82.61	1407.00
Sl-14	15517	943.782	82.533	1407.00
Sl-14	15822	1499.14	73.624	1407.00
Sl-14	16144	1441.518	82.608	1407.00
Sl-14	16194	1233.479	82.573	1407.00
Sl-14	16409	944.089	82.544	1407.00
Sl-14	16594	1498.211	73.61	1407.00
Sl-14	16736	944.297	82.54	1407.00

Sl-14	17178	1495.346	82.609	1407.00
Sl-14	17242	949.448	82.534	1407.00
Sl-14	17291	944.981	82.468	1407.00
Sl-14	17536	1497.621	73.612	1407.00
Sl-14	17588	1438.164	82.565	1407.00
Sl-14	18313	946.344	82.56	1407.00
Sl-14	18340	1438.71	82.576	1407.00
Sl-14	18794	1438.694	82.597	1407.00
Sl-14	18821	942.986	82.541	1407.00
Sl-14	19196	1498.502	73.602	1407.00
Sl-14	19337	1192.592	82.547	1407.00
Sl-14	19791	1441.533	82.615	1407.00
Sl-14	19852	946.745	82.52	1407.00
Sl-14	20197	1501.267	73.565	1407.00
Sl-14	20238	1439.698	82.588	1407.00
Sl-14	20306	1196.424	82.55	1407.00
Sl-14	20671	944.67	82.551	1407.00
Sl-14	20721	1499.978	73.598	1407.00
Sl-14	20741	1438.025	82.582	1407.00
Sl-14	20827	947.314	82.526	1407.00
Sl-14	21034	1438.799	82.564	1407.00
Sl-14	21233	1196.008	82.553	1407.00
Sl-14	21305	1441.758	82.568	1407.00
Sl-14	21656	1193.278	82.555	1407.00
Sl-14	21734	1444.18	82.588	1407.00
Sl-14	21785	1440.683	82.594	1407.00
Sl-14	22040	1439.64	82.601	1407.00
Sl-14	22188	1441.516	82.604	1407.00
Sl-14	22283	1469.552	73.626	1407.00
Sl-14	22652	1407.37	82.584	1407.00
Sl-14	22693	1441.746	82.582	1407.00
Sl-14	22784	948.928	82.552	1407.00
Sl-14	22971	1193.13	82.56	1407.00
Sl-14	23005	1440.274	82.579	1407.00
Sl-14	23412	1500.373	73.615	1407.00
Sl-14	23447	1438.98	82.567	1407.00
Sl-14	23793	1440.635	82.57	1407.00
Sl-14	24731	1439.982	82.598	1407.00
Sl-14	25369	1613.191	82.596	1407.00
Sl-14	27061	1445.458	82.548	1407.00

Table B.6. 20 Russian SL-16 Zenit-2 upper stages (3 May 2017)

Orbital stage of the launcher	USSTRATCOM catalog number	Mean altitude [km]	Inclination [deg]	Mass [kg]
SL-16	16182	836.192	71	9000.00
SL-16	17590	834.329	71.002	9000.00
SL-16	17974	832.667	71.009	9000.00
SL-16	19120	826.133	71.018	9000.00
SL-16	19650	837.77	70.997	9000.00
SL-16	20625	841.471	70.999	9000.00
SL-16	22220	835.359	71	9000.00
SL-16	22285	840.15	71.019	9000.00
SL-16	22566	840.59	71.007	9000.00
SL-16	22803	834.242	70.993	9000.00
SL-16	23088	841.408	71.001	9000.00
SL-16	23405	839.439	70.981	9000.00
SL-16	23705	840.016	71.017	9000.00
SL-16	24298	848.805	70.849	9000.00
SL-16	25400	804.196	98.485	9000.00
SL-16	25407	837.781	71.007	9000.00
SL-16	26070	838.703	71.005	9000.00
SL-16	27006	993.319	99.307	9000.00
SL-16	28353	842.966	71.002	9000.00

SL-16	31793	842.357	70.973	9000.00

Table B.7. 5 Russian SL-19 Rokot upper stages (3 May 2017)

Orbital stage of the launcher	USSTRATCOM catalog number	Mean altitude [km]	Inclination [deg]	Mass [kg]
SL-19	28061	900.082	99.48	1600.00
SL-19	32957	1347.676	82.498	1600.00
SL-19	35501	1352.916	82.496	1600.00
SL-19	36589	1038.978	100.524	1600.00
SL-19	37155	1344.651	82.462	1600.00

Table B.8. 6 Ukrainian SL-24 Dnepr-1 upper stages (3 May 2017)

Orbital stage of the launcher	USSTRATCOM catalog number	Mean altitude [km]	Inclination [deg]	Mass [kg]
SL-24	28367	932.878	98.237	2360.00
SL-24	33397	920.018	98.816	2360.00
SL-24	35688	981.937	98.123	2360.00
SL-24	36509	914.088	91.918	2360.00
SL-24	36600	987.056	98.301	2360.00
SL-24	37795	989.374	98.169	2360.00

Table B.9. 280 Russian SL-8 Kosmos upper stages (3 May 2017)

Orbital stage of the launcher	USSTRATCOM catalog number	Mean altitude [km]	Inclination [deg]	Mass [kg]
SL-8	1575	1435.341	56.125	1435.00
SL-8	1589	1536.208	56.05	1435.00
SL-8	2802	744.183	74.012	1435.00
SL-8	3048	690.728	74.005	1435.00
SL-8	3131	1190.38	74.052	1435.00
SL-8	3577	1186.486	74.047	1435.00
SL-8	3819	1184.564	73.99	1435.00
SL-8	4071	682.289	74.052	1435.00
SL-8	4139	681.916	74.035	1435.00
SL-8	4255	1146.272	74.021	1435.00
SL-8	4370	691.192	74.04	1435.00
SL-8	4391	1525.86	74.029	1435.00
SL-8	4579	689.8	74.004	1435.00
SL-8	4589	751.42	74.065	1435.00
SL-8	4784	973.622	74.033	1435.00
SL-8	4800	966.265	74.019	1435.00
SL-8	5051	977.23	65.814	1435.00
SL-8	5175	763.217	74.046	1435.00
SL-8	5181	1180.069	74.002	1435.00
SL-8	5218	1537.703	74.027	1435.00
SL-8	5239	983.608	74.027	1435.00
SL-8	5555	1560.411	74.018	1435.00
SL-8	5615	1191.754	74.033	1435.00
SL-8	5685	973.06	74.026	1435.00
SL-8	5707	760.272	74.028	1435.00
SL-8	5847	964.297	74.047	1435.00
SL-8	5907	1173.615	82.969	1435.00
SL-8	6020	965.89	74.019	1435.00
SL-8	6061	754.357	74.055	1435.00
SL-8	6125	1543.217	74.01	1435.00
SL-8	6149	950.866	82.971	1435.00
SL-8	6207	978.026	65.825	1435.00
SL-8	6271	1527.577	74.042	1435.00
SL-8	6320	1351.574	74.014	1435.00
SL-8	6324	745.097	74.079	1435.00
SL-8	6683	1538.027	74.023	1435.00
SL-8	6708	982.015	82.946	1435.00
SL-8	6826	1380.951	74.022	1435.00
SL-8	6829	971.319	82.944	1435.00

SL-8	6853	1551.506	74.001	1435.00
SL-8	6966	746.473	74.053	1435.00
SL-8	6993	1545.831	74.03	1435.00
SL-8	7009	972.291	82.949	1435.00
SL-8	7095	966.058	82.951	1435.00
SL-8	7273	1545.257	74.024	1435.00
SL-8	7284	1373.404	74.044	1435.00
SL-8	7350	969.298	82.946	1435.00
SL-8	7426	1384.603	74.062	1435.00
SL-8	7434	767.283	74.044	1435.00
SL-8	7443	1578.085	74.038	1435.00
SL-8	7477	982.097	82.945	1435.00
SL-8	7594	965.151	82.945	1435.00
SL-8	7665	1378.716	69.225	1435.00
SL-8	7686	1585.941	74.004	1435.00
SL-8	7737	959.798	82.989	1435.00
SL-8	7769	979.377	82.966	1435.00
SL-8	7831	1586.925	73.99	1435.00
SL-8	8073	975.473	82.902	1435.00
SL-8	8295	1581.22	74.011	1435.00
SL-8	8326	1176.277	82.96	1435.00
SL-8	8344	759.227	74.06	1435.00
SL-8	8421	972.605	82.977	1435.00
SL-8	8459	766.834	74.063	1435.00
SL-8	8597	978.504	82.971	1435.00
SL-8	8615	1586.894	74.054	1435.00
SL-8	8646	982.895	82.975	1435.00
SL-8	8874	979.216	82.966	1435.00
SL-8	8897	1585.633	73.999	1435.00
SL-8	8924	765.967	74.062	1435.00
SL-8	9013	1525.445	65.866	1435.00
SL-8	9023	757.617	74.045	1435.00
SL-8	9044	974.627	82.983	1435.00
SL-8	9062	966.831	82.933	1435.00
SL-8	9444	763.338	74.053	1435.00
SL-8	9510	969.774	82.94	1435.00
SL-8	9598	1572.6	74.014	1435.00
SL-8	9613	970.179	82.956	1435.00
SL-8	9638	967.423	82.939	1435.00
SL-8	9738	983.692	82.967	1435.00
SL-8	9848	976.949	82.955	1435.00
SL-8	10011	1537.97	65.867	1435.00
SL-8	10020	968.316	82.951	1435.00
SL-8	10121	770.104	74.051	1435.00
SL-8	10138	983.022	82.938	1435.00
SL-8	10142	966.024	82.971	1435.00
SL-8	10293	1567.745	74.028	1435.00
SL-8	10355	976.066	82.972	1435.00
SL-8	10461	972.558	82.954	1435.00
SL-8	10492	1183.284	82.921	1435.00
SL-8	10513	967.853	65.833	1435.00
SL-8	10521	753.813	74.028	1435.00
SL-8	10537	978.108	82.93	1435.00
SL-8	10591	1575.871	74.034	1435.00
SL-8	10600	966.576	82.935	1435.00
SL-8	10677	756.086	74.042	1435.00
SL-8	10693	970.296	82.989	1435.00
SL-8	10732	977.642	82.929	1435.00
SL-8	10745	966.263	82.933	1435.00
SL-8	10777	970.275	82.942	1435.00
SL-8	10918	970.76	82.916	1435.00
SL-8	10938	1583.722	74.02	1435.00
SL-8	10962	752.604	74.077	1435.00

SL-8	10992	968.589	82.93	1435.00
SL-8	11051	1588.268	74.046	1435.00
SL-8	11112	765.669	74.032	1435.00
SL-8	11136	1594.139	74.02	1435.00
SL-8	11170	1174.172	82.972	1435.00
SL-8	11239	975.961	82.934	1435.00
SL-8	11304	1572.436	74.042	1435.00
SL-8	11309	971.452	82.974	1435.00
SL-8	11321	973.629	82.928	1435.00
SL-8	11327	971.692	82.949	1435.00
SL-8	11379	970.217	82.945	1435.00
SL-8	11427	765.121	74.015	1435.00
SL-8	11511	766.885	74.04	1435.00
SL-8	11546	1580.678	74.021	1435.00
SL-8	11574	753.99	74.067	1435.00
SL-8	11586	964.698	82.941	1435.00
SL-8	11668	976.675	82.951	1435.00
SL-8	11681	977.421	82.932	1435.00
SL-8	11699	1579.106	74.015	1435.00
SL-8	11736	973.779	82.947	1435.00
SL-8	11751	972.936	65.84	1435.00
SL-8	11804	974.672	82.939	1435.00
SL-8	11870	766.557	74.05	1435.00
SL-8	11883	1573.391	74.014	1435.00
SL-8	12088	972.035	82.948	1435.00
SL-8	12092	971.824	82.94	1435.00
SL-8	12115	1452.488	73.988	1435.00
SL-8	12150	973.527	65.822	1435.00
SL-8	12298	973.432	82.954	1435.00
SL-8	12328	1574.494	74.025	1435.00
SL-8	12443	773.774	74.056	1435.00
SL-8	12508	974.134	82.961	1435.00
SL-8	12644	1564.385	74.028	1435.00
SL-8	12682	966.292	82.921	1435.00
SL-8	12792	764.569	74.026	1435.00
SL-8	12804	928.275	82.937	1435.00
SL-8	12836	973.497	82.914	1435.00
SL-8	12983	1569.771	73.982	1435.00
SL-8	13003	1716.578	82.952	1435.00
SL-8	13028	761.893	74.039	1435.00
SL-8	13034	977.715	82.937	1435.00
SL-8	13066	970.951	82.898	1435.00
SL-8	13111	975.83	82.927	1435.00
SL-8	13128	976.21	82.927	1435.00
SL-8	13149	771.974	74.04	1435.00
SL-8	13168	1577.827	74.051	1435.00
SL-8	13242	769.764	74.046	1435.00
SL-8	13260	982.88	65.834	1435.00
SL-8	13302	995.669	82.93	1435.00
SL-8	13354	965.144	82.965	1435.00
SL-8	13386	1585.63	74.007	1435.00
SL-8	13618	972.693	82.969	1435.00
SL-8	13649	765.808	74	1435.00
SL-8	13758	965.578	82.912	1435.00
SL-8	13769	1584.786	74.006	1435.00
SL-8	13917	972.424	82.941	1435.00
SL-8	13950	972.25	82.958	1435.00
SL-8	13992	769.064	74.054	1435.00
SL-8	14059	966.016	82.971	1435.00
SL-8	14085	974.253	82.94	1435.00
SL-8	14179	1564.406	74.022	1435.00
SL-8	14241	768.927	74.058	1435.00
SL-8	14402	769.847	74.045	1435.00

SL-8	14451	968.466	82.935	1435.00
SL-8	14547	971.319	82.928	1435.00
SL-8	14619	1569.412	73.998	1435.00
SL-8	14625	981.182	82.932	1435.00
SL-8	14680	973.445	82.959	1435.00
SL-8	14760	770.017	74.047	1435.00
SL-8	14966	980.599	82.97	1435.00
SL-8	14974	972.05	82.939	1435.00
SL-8	15006	1574.468	74.009	1435.00
SL-8	15032	773.71	74.07	1435.00
SL-8	15056	974.367	82.957	1435.00
SL-8	15078	971.194	82.951	1435.00
SL-8	15293	978.634	82.941	1435.00
SL-8	15360	972.64	82.941	1435.00
SL-8	15399	975.163	82.952	1435.00
SL-8	15483	768.894	74.047	1435.00
SL-8	15506	974.798	82.919	1435.00
SL-8	15598	973.176	82.934	1435.00
SL-8	15625	1591.042	74.056	1435.00
SL-8	15752	985.611	82.95	1435.00
SL-8	16012	768.668	74.062	1435.00
SL-8	16292	971.914	82.939	1435.00
SL-8	16369	972.437	82.943	1435.00
SL-8	16457	1586.972	73.987	1435.00
SL-8	16494	973.571	82.929	1435.00
SL-8	16511	975.973	82.945	1435.00
SL-8	16682	769.94	74.025	1435.00
SL-8	16728	972.835	82.959	1435.00
SL-8	16766	1575.095	74.011	1435.00
SL-8	16799	970.616	82.917	1435.00
SL-8	16864	754.642	74.031	1435.00
SL-8	16953	765.102	74.013	1435.00
SL-8	17067	969.412	82.948	1435.00
SL-8	17146	1574.465	74.017	1435.00
SL-8	17160	980.116	82.926	1435.00
SL-8	17240	982.412	82.933	1435.00
SL-8	17304	764.054	74.061	1435.00
SL-8	17360	972.84	82.916	1435.00
SL-8	17526	972.422	82.905	1435.00
SL-8	18096	767.873	74.04	1435.00
SL-8	18121	1579.344	74.008	1435.00
SL-8	18130	973.325	82.93	1435.00
SL-8	18161	971.789	82.932	1435.00
SL-8	18403	973.583	82.914	1435.00
SL-8	18586	766.865	74.009	1435.00
SL-8	18710	975.105	82.913	1435.00
SL-8	18945	1573.113	74.011	1435.00
SL-8	18986	965.89	82.956	1435.00
SL-8	19039	761.549	74.052	1435.00
SL-8	19257	764.896	74.047	1435.00
SL-8	19325	969.793	82.956	1435.00
SL-8	19770	760.335	74.043	1435.00
SL-8	19827	982.281	82.956	1435.00
SL-8	19910	1576.407	74.01	1435.00
SL-8	19922	971.013	82.957	1435.00
SL-8	20046	967.857	82.937	1435.00
SL-8	20104	970.836	82.961	1435.00
SL-8	20150	976.554	82.936	1435.00
SL-8	20433	769.36	74.038	1435.00
SL-8	20509	976.861	82.956	1435.00
SL-8	20528	986.661	82.934	1435.00
SL-8	20557	1576.617	73.984	1435.00
SL-8	20578	974.004	82.95	1435.00

SL-8	20805	975.995	82.936	1435.00
SL-8	21015	769.767	74.054	1435.00
SL-8	21088	971.573	82.946	1435.00
SL-8	21090	974.14	82.92	1435.00
SL-8	21108	1597.089	74.053	1435.00
SL-8	21131	960.409	82.832	1435.00
SL-8	21153	975.691	82.929	1435.00
SL-8	21231	976.19	82.947	1435.00
SL-8	21419	776.455	74.042	1435.00
SL-8	21667	978.551	82.911	1435.00
SL-8	21797	970.305	82.953	1435.00
SL-8	21876	976.75	82.925	1435.00
SL-8	21903	980.759	82.942	1435.00
SL-8	21938	977.852	82.936	1435.00
SL-8	21984	1580.561	74	1435.00
SL-8	22007	968.423	82.932	1435.00
SL-8	22081	778.155	74.044	1435.00
SL-8	22208	978.386	82.923	1435.00
SL-8	22308	976.331	82.938	1435.00
SL-8	22488	969.135	82.94	1435.00
SL-8	22591	970.354	82.931	1435.00
SL-8	22676	776.176	74.041	1435.00
SL-8	22889	968.654	82.947	1435.00
SL-8	23093	969.15	82.945	1435.00
SL-8	23180	968.31	82.943	1435.00
SL-8	23190	982.796	74.027	1435.00
SL-8	23432	777.826	74.036	1435.00
SL-8	23466	980.979	82.921	1435.00
SL-8	23527	984.063	82.945	1435.00
SL-8	23604	981.416	82.906	1435.00
SL-8	23774	973.616	82.985	1435.00
SL-8	24306	979.077	82.939	1435.00
SL-8	24678	983.72	82.936	1435.00
SL-8	24773	983.884	82.925	1435.00
SL-8	24955	955.766	82.917	1435.00
SL-8	25569	982.496	82.945	1435.00
SL-8	25592	982.068	82.932	1435.00
SL-8	25893	973.413	82.93	1435.00
SL-8	26819	976.938	82.923	1435.00
SL-8	27437	973.247	82.949	1435.00
SL-8	27466	1485.589	82.483	1435.00
SL-8	27535	981.102	82.934	1435.00
SL-8	27819	981.774	82.952	1435.00
SL-8	27870	1483.798	82.47	1435.00
SL-8	28381	967.441	82.963	1435.00
SL-8	28421	1485.63	82.481	1435.00
SL-8	28522	927.478	82.953	1435.00
SL-8	28910	1441.381	82.464	1435.00
SL-8	32053	974.433	82.975	1435.00
SL-8	33066	663.63	48.443	1435.00
SL-8	35637	921.416	82.96	1435.00
SL-8	36520	986.915	82.962	1435.00